Polymer Blends with Microfibrillar-Phase Morphology

Polymerní směsi s mikrofibrilární fázovou strukturou

Martina Polášková

Master Thesis
2006

Tomas Bata University in Zlín
Faculty of Technology

Univerzita Tomáše Bati ve Zlíně
Fakulta technologická
Ústav inženýrství polymerů
akademický rok: 2005/2006

ZADÁNÍ DIPLOMOVÉ PRÁCE

(PROJEKTU, UMĚLECKÉHO DÍLA, UMĚLECKÉHO VÝKONU)

Jméno a příjmení:	**Bc. Martina POLÁŠKOVÁ**
Studijní program:	**N 2808 Chemie a technologie materiálů**
Studijní obor:	**Inženýrství polymerů**
Téma práce:	**Polymer Blends with Microfibrillar-Phase Morphology**

Zásady pro vypracování:

The Master thesis will be focused on the possibilities of microfibrillar-phase formation in polymer blends during flow through extrusion die with semihyperbolic-converging channel. For these purposes, several blends of polyethylene and polypropylene will be prepared and used. Final structure of extruded blends will be examined at several structural levels using X-ray scattering, differential scanning calorimetry, electron microscopy and light microscopy. Finally, the effect of phase morphology on mechanical properties will be studied.

Rozsah práce:

Rozsah příloh:

Forma zpracování diplomové práce: **tištěná/elektronická**

Seznam odborné literatury:

TJONG, S.C. Mater. Sci. Eng. R 2003, vol. 41, p. 1.
TAYLOR, G.I. Proc. R. Soc. 1934, vol. A146, p. 501.
GRACE, H.P. Chem. Eng. Commun. 1983, vol. 14, p. 225.
MCHUGH, A.J. J. Appl. Polym. Sci. 1975, vol. 19, p. 125.
TUREK, D.E., SIMON, G.P. Polymer 1993, vol. 34, p. 2750.
MONTICCIOLO, A., CASSAGNAU, P., MICHEL A. Polym. Eng. Sci. 1998, vol. 38, p. 1882.
EHRENSTEIN, G.W., MAERTIN, C. Kunststoffe, 1985, vol. 75, p. 20.
OBADAL, M., ČERMÁK, R., STOKLASA, K., HABROVÁ, V. Plast. Rubb. Compos. Macromol. Eng. 2004, vol. 33, p. 295.
VARGA, J., BREINING, A., EHRENSTEIN, G.W. Int. Polym. Process. 2000, vol. 15, p. 53.
LI, X., CHEN, M., HUANG, Y., LIN, G., ZHAO, S., LIAO, B., WANG, C., CONG, G. Adv. Polym. Technol. 1997, vol. 16, p. 331.

Vedoucí diplomové práce: **Ing. Roman Čermák, Ph.D.**
Ústav inženýrství polymerů

Datum zadání diplomové práce: **29. listopadu 2005**

Termín odevzdání diplomové práce: **12. května 2006**

Ve Zlíně dne 7. února 2006

prof. Ing. Josef Šimoník, CSc.
děkan

L.S.

UNIVERZITA TOMÁŠE BATI VE ZLÍNĚ
Fakulta technologická

prof. Ing. Josef Šimoník, CSc.
ředitel ústavu

ACKNOWLEDGEMENTS

In the first place I would like to thank to my supervisor Roman Čermák for giving me opportunity to perform this work, his precious time, endless remarks and language corrections. Further, I am grateful to Mrs. Jiřina Dohnalová and Mr. Martin Zatloukal for their help in experimental part of this work and Mr. Petr Ponížil for his fruitful reminders. Finally, last but not least acknowledgments belong to my family and Mr. Tomaš Sedláček, who always supported me with valuable advices and inspirational suggestions.

I declare I worked on this Master thesis by myself and I have mentioned all the used literature.

Zlín, 11. 5. 2006 .....

Martina Polášková

ABSTRACT

The master thesis is focused on the possibilities of microfibrillar-phase formation in polymer blends during extrusion through a die with semihyperbolic-converging channel. For these purposes, three polyethylene/polypropylene blends with the mixing ratios (wt./wt.) 80/20, 70/30 and 60/40 were prepared. These blends as well as pure materials were described from the rheological point of view. Final structure and properties of extruded blends were examined using wide-angle X-ray scattering, differential scanning calorimetry, electron microscopy and tensile testing. It is demonstrated that the formation of microfibrillar-phase morphology is achieved in all the blends, independent of their mixing ratios and processing conditions used. However, the structure and properties of these microfibrillar-phase composites are strongly influenced by mixing/extrusion parameters.

Diplomová práce je zaměřená na možnosti vytlačování polymerních směsí s mikrofibrilární fázovou strukturou pomocí vytlačovací hlavy se semihyperbolickým sbíhavým kanálem. Za tímto účelem byly připraveny tři druhy směsí polyetylenu a polypropylenu ve hmotnostním poměru 80/20, 70/30, 60/40. Tyto směsi spolu s čistými materiály byly popsány z hlediska tokového chování. Výsledná struktura a vlastnosti vytlačených pásků byly následně studovány pomocí širokoúhlé rentgenografie, diferenciální snímací kalorimetrie, elektronové mikroskopie a tahových zkoušek. Práce ukazuje, že tvorba mikrofibrilární fázové struktury je dosažena ve všech směsích, nezávisle na mísících poměrech a zpracovatelských podmínkách. Nicméně, struktura a vlastnosti těchto mikrofibrilárních kompozitů jsou výrazně ovlivněné podmínkami míchání a vytlačování.

TABLE OF CONTENT

INTRODUCTION

Technical and financial incentives make polymeric materials an attractive alternative in an ever-increasing number of applications. The development of new resins, which, for several decades, attracted most of research effort, now tends to be supplemented by new approaches. The strength of these new tendencies is clearly shown by the rapid emergence of polymer blends and composites as engineering materials. In the case of blending, which represents a possible method for materials tailoring, desirable properties are mainly controlled through the miscibility of components employed. Actually, the miscibility is a critical factor determining rising phase structure, and consequently, overall properties (e.g. mechanical, thermal, rheological) of the blend.

Noteworthy, one of the greatest research interests in blending field has been dedicated to studies of properties and morphology of polyolefin blends. This is not only due to wide applicability of these materials in industry but rather due to their rich and fascinated morphology depending on molecular structure, thermal history, and external stress field. The melt-mixed compounds of polypropylene with polyethylene as a minor constituent are one of the most frequently studied blends in general. Their preparation was started especially with the intention of improving the low-temperature impact strength of polypropylene. Nevertheless, nowadays when plastic waste recycling is one of the main issues of environmental concerns, studies of polypropylene and polyethylene blends play important role, due to their consumed amount and difficult separation of these materials apart. Thus, it is important to study blends of polyethylene and polypropylene in order to put recycled blends into effective and efficient use.

Polymers compounding with special morphology governed by processing conditions, commonly known as in-situ composites preparation, offers extra possibilities of blend properties improving. Relatively successful in-situ composites preparation was achieved via blending of common thermoplastic resins with liquid crystalline polymers. Liquid crystalline polymers represent special macromolecular material containing rigid mesogenic units that in molten state keep defined conformation. During processing these rigid domains can be oriented along the flow which results in a fine fibril structure reinforcing the thermoplastic matrix. Besides this approach, in-situ composites were effectively prepared also from common polymeric materials several times cheaper than liquid crystalline polymers. One of such example is the combination of polypropylene with

polyamide 6. Nevertheless, only a few works dealt with improvement of mechanical properties of polyethylene by the polypropylene microfibrillar-phase reinforcement.

Present master thesis focuses on in-situ composites prepared by blending of two modelling materials, namely linear high-density polyethylene with isotactic polypropylene. Beside proper preparation of in-situ composites, interrelations between material composition, processing conditions and resulting structure and properties of polyethylene-polypropylene blends are studied.

1 POLYMER BLENDS

Blending of existing polymeric materials attracts considerable attention since it represents a method for combining the desirable properties of specific materials in the resultant system (1-3). Moreover, this approach is usually much more cost-effective way of the material properties tailoring then a totally new polymers preparation.

1.1 Preparation of blends

Two-phase polymer systems are usually prepared by a melt-compounding process. The properties of such systems may depend as much on the processing history as on the constituent base polymer and minor phase components. Single-screw extruders have long been used for compounding – the provision of homogenous mixtures as a result of the dispersive and distributive actions occurring within the extruder between screw and barrel. As a need for more sophisticated morphologies has developed, twin-screw extruders are finding increased usage because of the additional advantage of screw-to-screw interaction (4).

1.1.1 Compounding in twin-screw extruders

Twin-screw extruders are either co-rotating or counter-rotating, and either tangential or intermeshing. The intermeshing varieties may vary in the degree of intermesh to the point of being fully self-wiping. The main feature which distinguishes twin-screw from single-screw extruders is the interaction between the screws. Generally, the twin-screw extruders are starve-fed; a feature that provides independence between feed rate and screw speed, and thus an additional level of control over the compounding operation. The intermeshing twin-screw extruders have grooved or keyed shafts and a great variety of slip-on screw and kneading paddle sections that permit a seemingly endless variation of feeding, mixing, venting, and pressure generation arrays (4).

Furthermore the intermeshing counter-screw extruders are more efficient in pressure development (since conveying is positive and not dependent upon drag flow). As such, there is less product temperature rise, which is critical for temperature-sensitive polymers. The high pressures can be generated at low screw speeds. Absence of an easy leakage path minimizes pressure flow, making these extruders ideal for profile extrusion.

Intermeshing counter-screw extruders used for compounding tend to be longer and operate at higher screw speeds. Thiele (5, 6) described the features that may offer particular advantages in compounding. The feed flight channel width can be selected not only to provide easy positive feeding, but also to control the degree of fill in subsequent downstream channels (with lower helix angels).

Although material is conveyed in closed C-shaped flight chambers down the barrel, mixing does arise from the circulation pattern generated in the C-shaped chamber, and by the leak flows over the flights and between the screws. Janssen (7) has described these leakage flows in detail. The flow in the calendar gap between the two screws is particularly effective for dispersive mixing.

The material subjected to calendar gap dispersion is remixed in C-chamber. A given level of dispersion capability is achieved without high heat generation. Additional shearing can be provided with overlapping blister rings. When these are serrated, they are similar to the gear homogenisers used in co-workers (8) have modelled the flow patterns in the calendar gap by finite element analysis. A vortex may form at the entry, but its presence is determined uniquely by the relative leakage flow.

1.2 Extrusion of blends

Extrusion is one of the possibilities how to process polymer blends. In principle the extrusion consists of metering polymer (usually in granular form) into a heated barrel in which a screw is rotating. The rotation of the screw causes the granules to move up the barrel, where they are compacted and plasticized. The resultant melt is then forced under pressure through an orifice to give a product of constant cross-section. Nevertheless it is very difficult to generalize this process since blends are generally more sensitive to process variables (e.g., stress, temperature, pressure, and residence time) and need more sophisticated line control than a single-phase polymers (4).

All blends can be grouped into two types: well stabilized and not. In the first type the processability is similar to single-phase polymer. The second, nonstabilized morphology type includes blends designed to create particularly desirable structures during the final processing step. This includes blends used to manufacture e.g. blow-moulded containers with superior barrier properties, or strong microfibrillar-phase reinforced profiles (4).

1.2.1 Single-screw extruder

A single-screw extruder (Fig. 1.1) consists of a screw in a metal cylinder or barrel. One end of the barrel is attached to the feed throat while the other end is open. A hopper is located above the feed throat and the barrel is surrounded by heating and cooling elements. The screw itself is coupled through a thrust bearing and gearbox, or reducer, to a drive motor that rotates the screw in the barrel. A die is connected to the "open" end of the extruder with a breaker plate and screen pack (or a screen changer) forming a seal between the extruder and die (9).

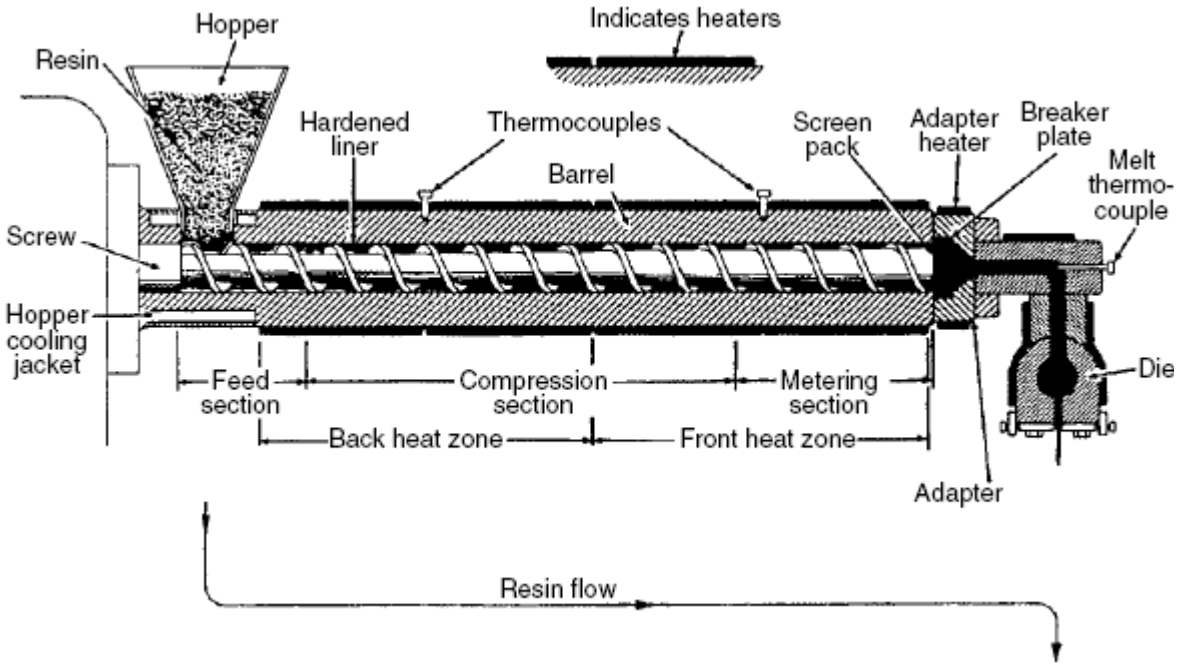

Fig. 1.1. Single-screw extruder (9).

Although barrel and barrel liners typically have smooth surfaces, a liner or barrel with axial grooves can be installed in the feed section of the extruder (Fig. 1.2). Groove depth is greatest at the feed throat and gradually decreases with axial distance. Since the grooves increase shear, friction, and pressure, they improve extruder output. However, the feed section requires additional cooling, thermal insulation must be installed between the grooved section and the rest of the barrel, the feed zone must also be able to withstand higher pressures (typically 100 to 300 MPa) (9).

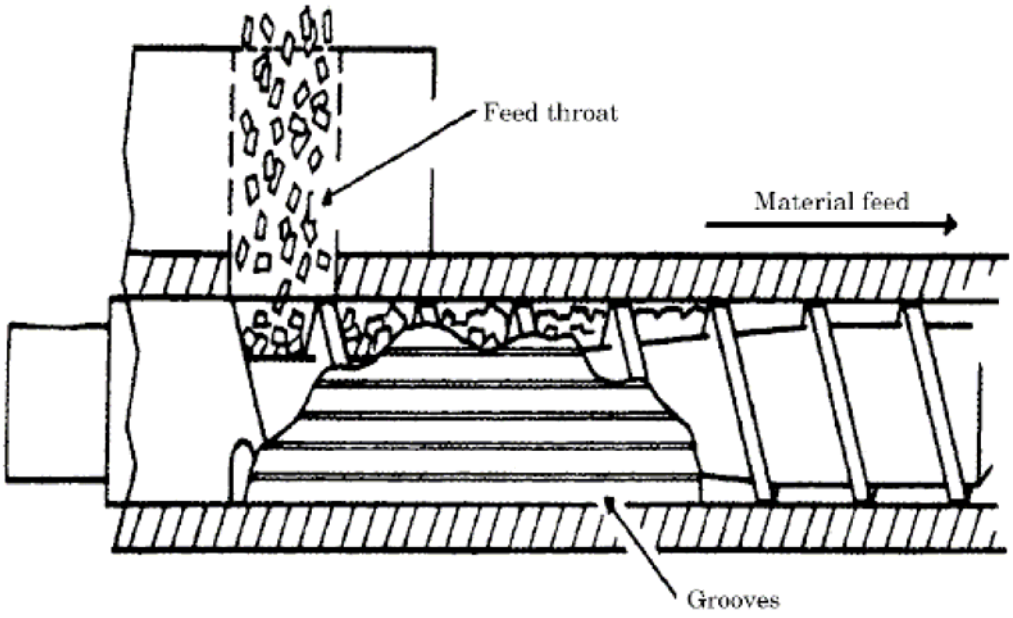

Fig. 1.2. Grooved-barrel liner (9).

1.2.2 Gear pump

Within the past several years considerable interest has developed in retrofitting single screw extruders with gear pumps. Fig. 1.3 is a scheme of gear pump, which is usually attached directly to the discharge end of the extruder and delivering high-pressure melt to the downstream forming devices (10).

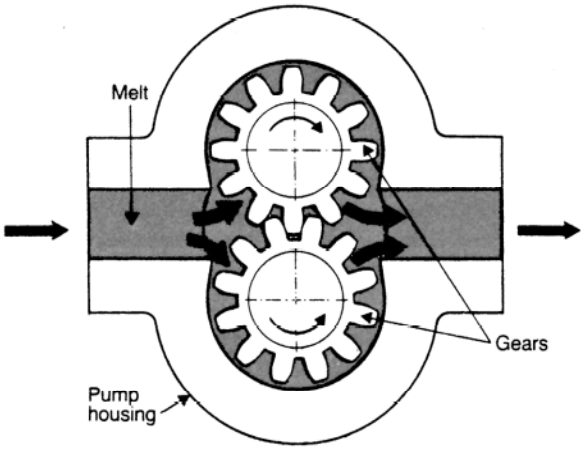

Fig. 1.3. Scheme of gear pump (10).

The motivation for installing gear pumps has been to increase the uniformity of flow from the extruder and, hence, to improve the dimensional uniformity of extruded product. In general, extrusion rate variations of less than 1 % are easily obtained with gear-pump-

equipped extruders. Pump-assisted extrusion has therefore found applications in wire coating, profile extrusion, and other processes where dimensional uniformity is an important consideration (10).

In addition to extrudate uniformity, pump-assisted extrusion offers the possibility of increased rate, lower extrudate temperature, and improved energy efficiency for the process. Whether or not these additional benefits will be obtained depends on the initial performance of the extruder and on the specifics of the screw selected to work with the pump (10).

1.2.3 Extrusion die

A die is a device, usually made of steel, having a specific shape or design geometry which it imparts to a plastic melt pumped from an extruder. The function of the die is to control the shape of the extrudate. The important word is control. In order to do this, the extruder must deliver melted plastic to the die targeted to be an ideal mix at a constant rate, temperature, and pressure. Measurement of these variables is desired and usually carefully performed (10).

The terms die, tool, and mould are virtually synonymous in the sense that they have female or negative cavity through which a molten plastic moves usually under heat and pressure. However, the term die principally refers to an extruder die in the plastic industry. The design of a die is required to: (i) minimize head and tooling interior volumes to limit stagnation areas and residence time; (ii) streamline flow through the die, with low approach angles in tapered transition sections; and (iii) polish and plate interior surfaces for minimum drag and optimum surface finish on the extrudate (10).

Basically, the die provides the means to “spread” the plastic being processed under pressure to the desired width and thickness in a controllable, uniform manner. In turn, this extrudate is delivered from the die (targeted with uniform velocity and uniform density lengthwise and crosswise) to take-off equipment in order to produce a shaped product (film, sheet, pipe, profile, coating, filament, etc.) (10).

1.3 Control of blend properties

McKelvey defined plastics processing as “operations carried out on polymeric materials or systems to increase their utility”. These types of operations produce flow, chemical

change, and/or a permanent change in physical properties (11). From the blends processing point of view, it is well known that the final properties of blends are strongly affected by shape and size of dispersed phase, at the same time, variety of shapes (e.g. spheres, fibrils, or plates) can be formed. Which of these phase structures is preferential-formed depends on the weight ratio of the blend components, their chemical structure, properties, and processing conditions (4).

1.3.1 Miscibility

In spite of obvious advantages, polymer blends are accompanied by problems resulting from immiscibility of majority of polymer pairs. In fact, the level of miscibility is a critical factor determining phase structure and overall properties (e.g. mechanical, thermal, rheological) of the blend. Thus one of the most basic questions in blends is whether or not the two polymers are miscible or exist as a single phase (9).

Although miscible blends of polymers exist, most blends of high molecular weight polymers are immiscible. Thus, when polymers are mixed together, the blend components are likely to separate into discrete phases. This characteristic, often combined with low physical attraction forces across the phase boundaries, causes immiscible blend systems to have poor mechanical properties (12, 13). In principle, an unambiguous criterion of the miscibility can be assessed.

Miscible systems show unlimited solubility and zero interfacial tension, therefore a mixture of the components is expected to result in homogenous blend. However, a limited mutual solubility and finite interfacial tension, in majority cases occur in polymer blending, result in two-phase structure – immiscible system (4).

In the case of a miscible single-phase blend there is a single glass transition temperature (T_g), which is dependent on the composition of the blend (14). Where two phases exist, the blend exhibits two separate T_g values, one for each of the phases present.

In the case where the polymers can crystallize, each crystalline portion will exhibit a melting temperature (T_m), even in the case where the two polymers are a miscible blend.

In general, miscibility of any mixture is governed by thermodynamics of the interactions between the components, reflecting their physical and chemical structures (15).

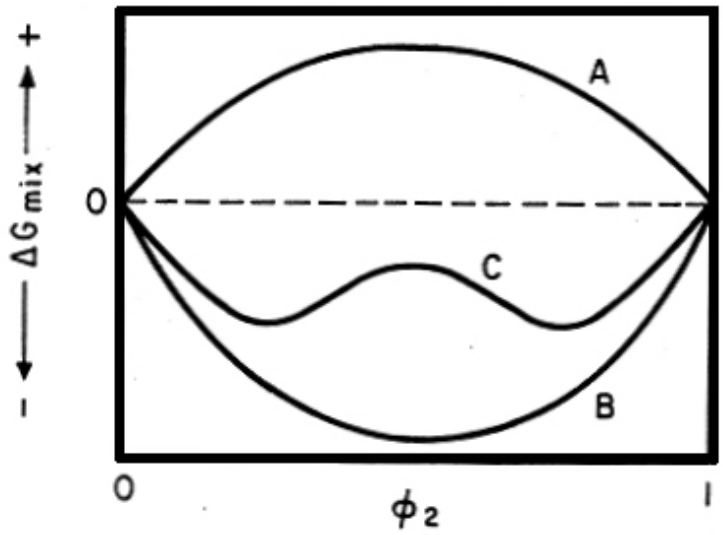

Fig. 1.4. Possible free energy of mixing for binary systems.

The basic rule thermodynamically defines the state of miscibility in the view of Gibbs free energy of mixing as

$$\Delta G_m = \Delta H_m - T \cdot \Delta S_m < 0 \qquad (1.1)$$

where ΔG_m is free energy of mixing, ΔH_m is the enthalpy change of mixing, ΔS_m is the entropy change of mixing, and T is the temperature. As shown in Fig. 1, ΔG_m for a binary mixture can vary with composition in several ways.

For complete miscibility, free energy of mixing must be negative, and at the same time the second derivative of free energy with composition must be positive (12)

$$\left(\frac{\delta^2 \Delta G_m}{\delta \phi_2^2} \right)_{T,p} \rangle 0 \qquad (1.2)$$

where ϕ_2 stands for the volume fraction of the second component.

Referring back to Fig. 1.4, these criteria are met by curve B for all compositions. In this case, blend components are truly miscible, which is among others reflected in the homogeneity at the molecular level, and the observation of a single glass transition temperature. Blends described by curve A, on the other hand, violate relation 1, and are completely immiscible. A system described by curve C is partially miscible; a single amorphous phase can be formed in compositions to the left and right of the minima of curve C. Two phases will be formed, however, with compositions given by the minima when mixtures are blended at overall concentrations in the central range (16).

1.3.2 Compatibilisation

Compatibility of immiscible components can be attained in the following ways (17):

- By adding a third compatibilising component (e.g. block or graft copolymer) with segments capable of specific interactions and/or chemical reactions with at least one of the blend components. Copolymers may be considered as true "interfacial agents" since they tend to concentrate and act at the interface as emulsifiers;
- By blending suitably functionalised polymers capable of enhanced specific interactions and/or chemical reactions. In the reactive system, copolymers may be formed in-situ during mixing, and since they have segments chemically identical to those in the respective unreacted homopolymers, they are thought to be located preferentially at the interface. Thus, they may be considered equivalent to the block or graft copolymers that are added separately.

With respect to blends of polyolefins (PO) and polyesters, especially reactive melt blending is employed to overcome their immiscibility resulting from the different chemical structure and polarity. The basic principle lies in the functionalisation of polyolefin with a polar monomer, which leads to a formation of grafted PO with increased polarity and affinity with other polar materials.

Generally, the main role of compatibiliser, usually concentrating at the interface during blending, is to reduce interfacial tension, prevent coalescence, and enhance interfacial adhesion (3, 13, 18). As a result, the domain size decreases and the mechanical properties improve. Another important function is to serve as a processing aid or lubricant in reducing viscosity of the blend, since low viscosity improves mixing.

(a) (b)

Fig. 1.5. Scheme of binary blend without (a) and with (b) compatibiliser (16).

The comparison of the situation before and after addition of compatibiliser is depicted in Fig. 1.5. As can be seen, compatibiliser acts as a bridge that couples the two distinct phases; in other words, it creates an interphase region where the interpenetration of the polymeric chains from both components is thermodynamically favourable (16).

1.3.3 Phase structure of polymer blends

Besides compatibilisation, an effective tool to prepare blends with satisfactory performance is a proper control of the phase structure (19). The morphology of heterogeneous systems depends on the composition (volume fractions), rheology of the components (viscosity and elasticity), their interactions (interfacial tension), and on the degree of mixing (deformation and thermal histories).

With reference to a number of influencing factors and their interrelations, it is not surprising that except for rather contradictory results, general rules for predicting the dependence of the phase structure on the blend composition have not been found yet. Consequently, only approximate descriptions from the theoretical point of view, and investigations under simplified conditions (simple flows, using Newtonian liquids instead of viscoelastic ones, etc.) are available (20).

In general, important aspects characterizing the phase structure are its type and fineness. Regarding the former, dispersed or co-continuous morphologies are generally distinguished. The dispersed-phase structure is represented by the particles of the minor phase dispersed in the major one. As the concentration of the minor phase increases, co-continuous structure is formed. Finally, at high concentrations of originally minor phase, phase inversion takes place. Comparing to low-molecular emulsions, where relatively sharp transition is defined, the definition of phase inversion in the case of polymer blends is more difficult since it is affected by the viscosities of both components. In general, the composition interval where one type of phase structure changes into another is broader (16).

So far, the fineness of phase structure has been investigated in particular for disperse morphologies. In this case, the size of dispersed droplets is controlled by the competition between their breakup and coalescence (21-23) during mixing, and in principle can be solved by the equation relating both processes. However, only approximate results are available, predominantly for the steady state, when the dynamic equilibrium is achieved.

1.4 In-situ composites

Processing of an incompatible polymer pairs during which the dispersed phase forms in-situ reinforced fibres is the preferable way to achieve the highest mechanical properties of polymer blends (24).

1.4.1 LCP in-situ composites

Blending of thermotropic liquid crystalline polymers (LCP) with commodity thermoplastics is an exemplary mean of the mechanical properties improvement. LCPs with high strength and stiffness, high chemical resistance, good dimensional stability and low linear thermal expansion coefficient are attractive high performance engineering materials (25).

LCPs consist of repeating stiff mesogenic (liquid crystalline) monomer units that are incorporated either in the main-chain or in side chain of polymer backbone. The mesogenic molecules are highly anisotropic in terms of the optical, rheological, electrical and magnetic properties. Since LCPs, due to the high cost of the monomer synthesis and polymerisation, are far more expensive than the general-purpose engineering plastics, it is much more cost effective to create polymer composites with superior mechanical performance using LCP as a minor blending component (25).

From the processing point of view, since the LCP has lower viscosity at processing conditions, it acts as a processing aid reducing the viscosity of thermoplastic matrix during compounding, thereby easing the processability of thermoplastics. Moreover, during flow of two-phase systems the low-viscosity component migrates (4) (due to process kinetic depending on the stress gradient, as well as the relative viscosity and normal stress of the components) towards the high stress domain, e.g., lubricating the flow through pipes, runners, dies and capillaries (26).

Further important factor playing key role in preparing of LCP in-situ composites is a high degree of long-range order in the mesogenic phase. These, e.g. nematic units, can orient along the flow direction during processing. It leads to the formation of fine fibrils at an appropriate range of LCP concentration under certain processing conditions. The fine fibrils reinforce the matrix of the thermoplastics effectively, giving rise to the development

of polymer composites, commonly known as in-situ composites. In this regard, in-situ composites are akin to short-fibre-reinforced thermoplastic composites (25).

It is well accepted that the mechanical strength and stiffness of polymer are improved considerably with the incorporation of short glass-fibre reinforcement. However, conventional polymer composites reinforced with higher volume content of glass fibres are generally difficult to process owing to their high melt viscosity. Other difficulties encountered in short glass-fibre reinforced polymer composites include wear of processing facility resulting from the abrasion of reinforcement and fibre breakage. Thus, in-situ composites are considered to be competitive with glass-fibre reinforced polymers where processability and low density are dominant requirements (25).

While the LCPs are often too expensive for general engineering applications, there are considerable supplies of engineering plastics in the form of post-consumer scraps, which are low cost source of raw materials for polymer blend forming. But, opposite to LCPs, the molecules of common thermoplastics relax during melt processing; therefore a good molecular orientation is almost impossible. In order to overcome this problem, a new type of processing route, the so-called microfibrillar-reinforced composite (MFC) concept was created several years ago (27-29).

1.4.2 Microfibrillar-reinforced composites

The preparation of MFC includes three basic steps:

- Melt blending with extrusion of two immiscible polymers having different melting temperatures T_m (mixing step);
- cold drawing of the extrudate with good orientation of the two phases (fibrillization step);
- thermal treatment at temperature between the T_m of the two blend partners (isotropisation step).

While during the second step the two polymers are converted into highly oriented state, i.e. one deals with an oriented blend (30), the third step results in melting of lower melting component and its transformation into an isotropic matrix, reinforced with the microfibrils of the higher melting component. Technologically, this transition to an MFC structure can take place during processing of the drawn blend via injection or compression moulding.

The processing window placed rather far from T_m of the microfibrils is the essential requirement, otherwise the microfibrils will melt and returned into a spherical shape (24).

Generally, there are two important factors typical for composite materials contribute to good mechanical property profile: (i) a higher aspect ratio, and (ii) a good adhesion between the matrix and the reinforcing phase. In fact, it was demonstrated in studies (27-30) that in the case of MFC from condensation polymers chemical linkages arising from transreaction and additional condensation reactions improve the adhesion between the two components. In the cases where chemical interactions are not possible, a strong nucleation effect of microfibrils on the matrix crystallization, i.e. the formation of transcrystallization layers can sometimes help to strengthen the fibre/matrix adhesion (31-33).

An example of MFC could be seen in Fig. 1.6, which shows longitudinal sections of strained and quenched strands of the model system polystyrene/high-density polyethylene formed after leaving the die of a co-rotating twin-screw extruder. Fig. 1.6a shows a beautiful MFC structure, as a result of immediate quenching of strained strand after die outlet. On the other hand, disintegration of the thinner threads into lines of droplets, shown in Fig. 1.6b, is caused by extension of the same strand after only a few seconds residence in the circumventing air (by increasing somewhat the distance between the die and the water bath) (34).

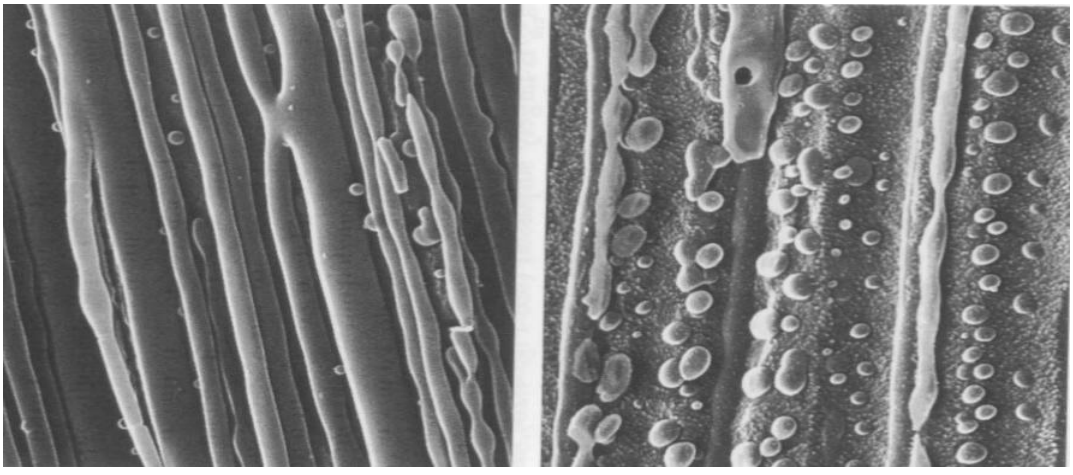

(a) (b)

Fig. 1.6. Breaking polystyrene threads in a high-density polyethylene matrix. The blends were prepared using a co-rotating twin-screw extruder with (a) quenching several seconds between die and water bath or (b) immediately after die (34).

Contrary to above-mentioned technique of MFC preparation, in present work possibility to achieve the same reinforcing effect using different process and material is investigated. Fibrillar structure is already created during extrusion and the structure is fixed in the die by cooling at temperature close to T_m of higher melting component. Since the extrudate leaving the die is intensively cooled, MFC structure can be successfully prepared also in one processing step.

2 POLYETHYLENE AND POLYPROPYLENE

2.1 Polyethylene

Polyethylene has the simplest basic structure of any polymer, it is the largest tonnage plastics material, and it is a polymer about which more as probably has been written than any other. The main attractive features of polyethylene, in addition to its low price, are excellent electrical insulation properties over a wide range of frequencies, very good chemical resistance, good processability, toughness, flexibility and, in thin films in certain grades, transparency (35).

Generally polyethylene is a wax-like thermoplastic with the chemical formula:

$CH_3 – (CH_2)_n – CH_3$

where n typically is in the range of 10^3-10^6. In the technical literature the term high-density polyethylene is used for this linear polyethylene while the term low-density polyethylene is used for branched polyethylene. It should be mentioned that the following investigation is focused on linear high-density polyethylene (PE). Its melting temperature is at 138 °C, but the exact value depending on the detailed molecular structure. Generally low values of melting temperatures are to be expected of a structure with a flexible backbone and no strong intermolecular forces. Glass transition temperature is between -128 °C and -30 °C, depending on the history of the sample and the experimental method used.

Polyethylene was for a long time used as a model polymer for morphological studies of semicrystalline polymers because of its simple chemical structure. Macromolecule chains occupy trans conformation (zigzag) (Fig. 2.1) that is the form with the lowest potential energy. So the crystals are composed of PE macromolecules in the all-trans conformation (36).

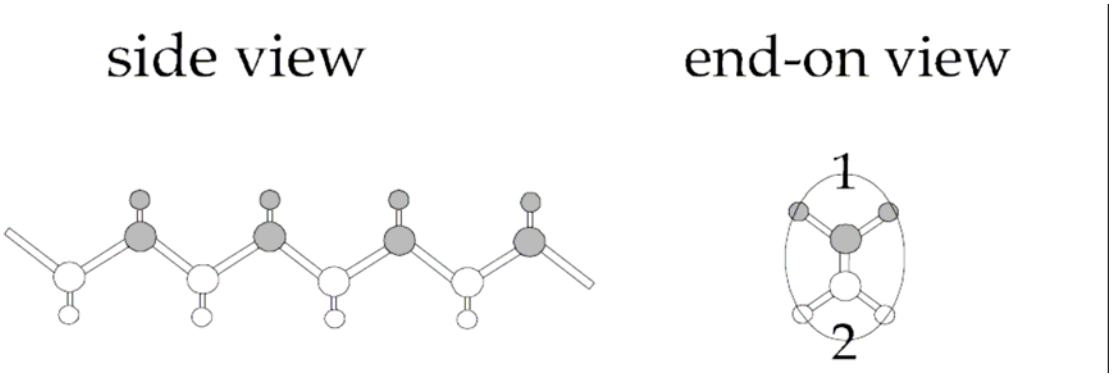

Fig. 2.1. The all-trans conformation (zigzag) of PE. Side and end-on view. The carbon atoms are large and hydrogen atoms are small. The shading is chosen in order to outline the difference in height between sides 1 and 2 (36).

When PE is crystallized from a supercooled solution or the melt, the chains are organized by folding to form lamellae (37, 38) (the growth of thin lamellar crystals with chain folding is a general phenomenon for crystalline polymers). These rapidly branch to form more complicated, filling space in 3 dimensions to form a ball-like structure known as a spherulite (39). Depending on the molar mass and crystallization temperature, PE forms different kinds of superstructures. The more common morphologies observed include:

- Faceted single lamellas containing folded or extended chains
- Nonfaceted lamellas
- Branched (dendritic) structures
- Sheaf-like arrays of lamellar ribbons (axialites, hedrites)
- Spherulitic arrays of lamellar ribbons (spherulites)
- Fibrous structures
- Epitaxial lamellar overgrowths on microfibrils (40)

Normally PE crystallizes in the orthorhombic crystalline form. The orthorhombic PE crystalline unit cell has the following cell dimensions: a = 7.40 Å, b = 4.94 Å and c = 2.534 Å. It was found that under extreme conditions, like for example crystallization with extreme cooling rates or crystallization under stress, PE can crystallize also in the monoclinic form. The monoclinic PE crystalline unit cell has the following cell dimensions: a = 8.09 Å, b = 2.53 Å, c = 4.79 Å and β = 107,9° (36).

The mechanical properties are strongly dependent on the molecular weight and on the degree of branching of the polymer. As with other polymers these properties are also dependent on the rate of testing, the temperature of test, the method of specimen preparation, the size and shape of the specimen and, to only a small degree with polyethylene, the conditioning of specimens before testing (35).

The main mechanical characteristics of PE are summarized as follows (35):

- Elongation at break: 20–800 %
- Tensile strength: 22–27.5 MPa
- E-modulus: 700-1400 MPa
- Izod impact strength: 2–6.8 J

2.2 Polypropylene

Polypropylene is a versatile thermoplastic material, compatible with many processing techniques and used in many different commercial applications. It is one of the fastest growing classes of commodity thermoplastic. The moderate cost and favourable properties of polypropylene contribute to its strong growth rate (41).

Propylene is an unsaturated hydrocarbon, containing only carbon and hydrogen atoms with chemical formula: $CH_3 - (CH_2 - \underset{\displaystyle |}{CH})_n - CH_3$ with a large n.
$\qquad\qquad\qquad\qquad\qquad\qquad\qquad\qquad\qquad\quad CH_3$

Tacticity of polypropylene is defined by the stereochemistry of the pending methyl group (CH_3). Polypropylene may be synthesised in three different forms: isotactic, syndiotactic and atactic (Fig.2.2). In the present work, isotactic polypropylene (PP) is used. By definition all repeat units of isotactic polypropylene are geometrically identical. Because of its structure, isotactic polypropylene has the highest crystallinity, resulting in good mechanical properties such as stiffness and tensile strength. The melting temperature of isotactic polypropylene is at 171 °C and the glass transition temperature (42) between 30 °C and 20 °C, depending on sample history and experimental method used.

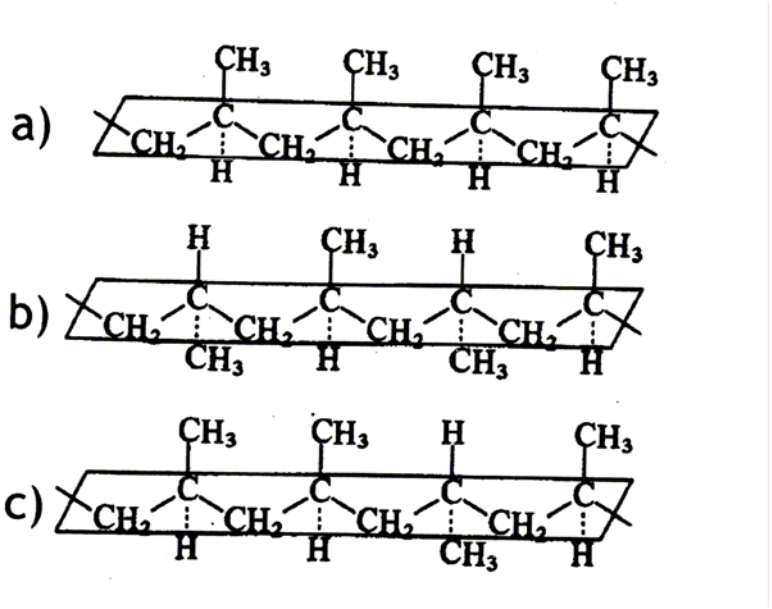

Fig. 2.2. Stereo-configurations of propylene sequences: a) isotactic; b) syndiotactic; c) atactic (43).

It is known that PP may crystallise in three different crystalline forms: α (monoclinic), β (hexagonal) and γ (triclinic). Crystalline forms of PP are composed of PP 3_1 helices (Fig. 2.3).

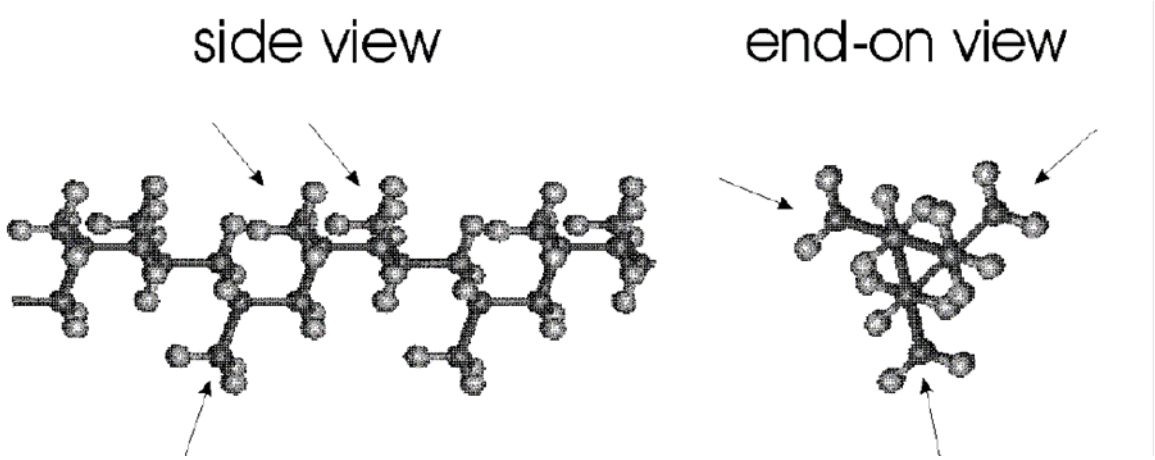

Fig. 2.3. The helical form of PP macromolecule. On the side view two helical turns are presented. Arrows show three methyl groups along one helix (36).

Mechanical properties of polypropylene are strongly dependent on its crystallinity. Increasing crystallinity increases stiffness, yield stress, and flexural strength but decreases toughness and impact strength. The secant flexural modulus at 1 % displacement can range from 2067–2412 MPa for polypropylene with ultra-high crystallinity but decreases to 1378–1654 MPa for general-purpose polypropylene of lower crystallinity (44, 45).

Polypropylenes generally have higher tensile, flexural, and compressive strength and higher moduli than polyethylenes due to the steric interaction of the pendant methyl groups, which result in a more rigid and stiff polymer chain than in polyethylene.

2.3 PP/PE blends

It is well known that PE and PP are immiscible polymers. The term "immiscible" means that the Gibbs energy of mixing is positive, thus two immiscible components tend to macroseparate from their mixture. The immiscibility of PE and PP was established by directly visualising macroseparation in the blend of molten PE and PP. A thin film of blended PE and PP was placed between two heated glass slides and observed with light microscopy. It was shown that initially small domains of PE and PP tend to merge leading finally to macroseparation of both polymers. Despite of the immiscibility of many polymers it is possible to produce their blends. Because of the high viscosity of bulk polymers the process of macroseparation takes place on a long time scale. By extrusion of two immiscible molten components and following fast cooling below crystallization or glass transition points of both components it is possible to prevent them from macroseparation. It is clear that properties of a blend of two immiscible components would strongly depend on the preparation conditions like, for example on the mixing and cooling rates. In general, immiscible polymers are also incompatible. The term "incompatible" means that the mechanical properties such as impact strength, Young's modulus, strain and elongation at the stretching limit of the blend are inferior to the mechanical properties of the pure components (36).

Despite the immiscible nature of PE and PP it is possible to process blends of PE and PP with impact strength of the blend which is two times higher than that of the pure components. It is important for industrial applications that by blending of common and cheap polymers one can obtain blends with improved impact strength. The blend of PE and PP with improved impact strength is processed by extrusion of both molten components, followed by fast cooling. Transmission-electron microscopy images of the blend show that these preparation conditions lead to a fine micro-separation of PE and PP, hence to an increased total interfacial area between PE and PP in their blend. Then, the enhanced total interfacial area improves the impact performance of the blend (36).

According to literature it is supposed that the "cross hatched" morphology of PE and PP established by epitaxial crystallization of PE on PP is responsible for the improved mechanical properties of PE and PP blends. Lamellae of PE grow epitaxially at about 50° with respect to the orientation of PP lamellae. As a consequence, PE lamellae join lamellae of PP and vice versa, which leads to hardening of the PE/PP blend (Fig. 2.4).

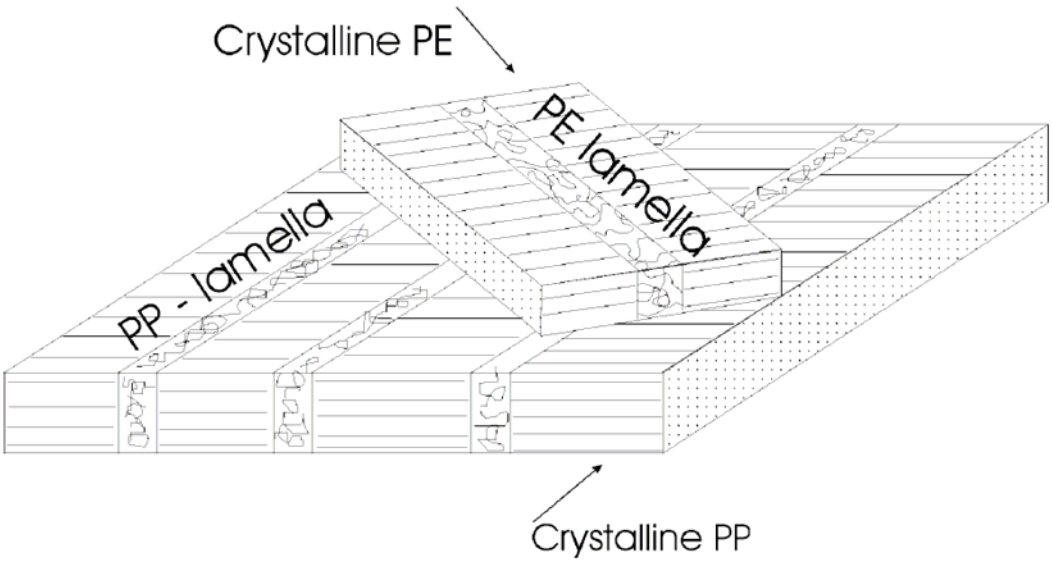

Fig. 2.4. Bridging mechanism established by epitaxial crystallization. It was found that lamellae of PE form an angle of about 50° with PP lamellae. This figure shows the bridging of several PP lamellae by PE lamellae (36).

3 EXPERIMENTAL METHODS

Following paragraphs deal with analysis methods that were employed for structural, mechanical and rheological characterizations of prepared samples.

3.1 X-ray diffraction

X-ray diffraction is a traditional method of crystallographic structure determination, and, as the standard techniques, it can be also used in the study of crystalline polymers. X-ray measurements are mostly used to determine the degree of crystallinity and orientation of polymeric systems (46).

Diffraction is the result of radiation's being scattered by a regular array of scattering centres whose spacing is about the same as the wavelength of the radiation. Scattering occurs when a photon of electromagnetic radiation interacts with an orbital electron in the atom. A single atom scatters an incident beam of X-ray in all space direction. A crystal (a large number of atoms arranged in a perfectly periodic array in three dimensions) acts as a three-dimensional diffraction grating. For diffraction to occur, the diffracted X-ray beams should be in constructive interference (47).

The diffraction pattern obtained when X-ray beam impinges on a polymer depends on the crystallinity. Large changes in intensity (with a small change in scattering angle at various mean scattering angles) are associated with the crystallites, while a broad, less intense band is characteristic of the amorphous portion (47).

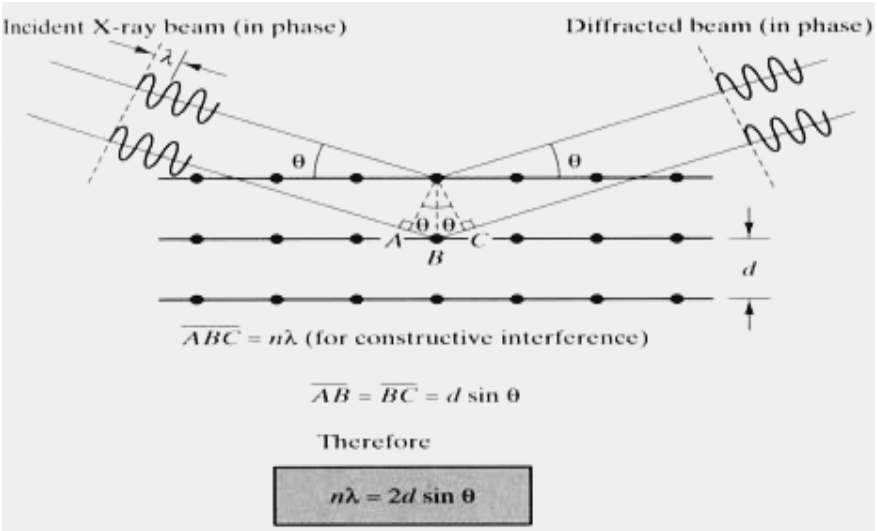

Fig. 3.1. Scheme of X-ray diffraction and Bragg's equation definition (47)

X-ray diffraction gives no information about the location of crystals, but the information that it gives about the range of orientations in the irradiated volume can be used with scanning electron microscopy to build up a picture of the microstructure.

3.2 Electron microscopy

Electron microscopes were developed due to the limitations of light microscopes which are limited by the physics of light to 500x or 1000x magnification and a resolution of 0.2 micrometers. In the early 1930's this theoretical limit had been reached and there was a scientific desire to see the fine details of the interior structures of organic cells (nucleus, mitochondria etc.). This required 10.000x plus magnification which was just not possible using light microscopes (48).

The transmission electron microscope was the first developed type of electron microscope. It is patterned exactly on the light transmission microscope except that a focused beam of electrons is used instead of light to "see through" the sample. It was developed by Max Knoll and Ernst Ruska in Germany in 1931. The transmission electron microscope works much like a slide projector. A projector shines a beam of light through (transmits) the slide, as the light passes through it is affected by the structures and objects on the slide. These effects result in only certain parts of the light beam being transmitted through certain parts of the slide. This transmitted beam is then projected onto the viewing screen, forming an enlarged image of the slide. The transmission electron microscope works the same way except that they shine a beam of electrons (like the light) through the sample (like the slide). Whatever part is transmitted is projected onto a phosphor screen for the user to see (48).

The first scanning electron microscope debuted in 1942 with the first commercial instruments around 1965. Its late development was due to the electronics involved in “scanning” the beam of electrons across the sample. This beam travels downward through a series of magnetic lenses designed to focus the electrons to a very fine spot. Near the bottom, a set of scanning coils moves the focused beam back and forth across the sample, row by row. As the electron beam hits each spot on the sample, secondary electrons are knocked loose from its surface. A detector counts these electrons and sends the signals to an amplifier. The final image is built up from the number of electrons emitted from each spot on the sample.

The scanning electron microscope is suited to most types of surface morphology examination especially for studying of fracture surface but also much interest centres on the surface of polymer fibres because it controls most of their important properties. Polymer fibres are typically 10-20 μm in diameter and often contain fibrils and microfibrils that are much finer still. As a consequence they are very easily damaged in the electron beam, even when coated with metal. It is difficult to dissipate beam-induced heat and the consequent temperature rise may cause expansion and hence movement during observation, adding a further difficulty that can usually be overcome with combination of well-executed coating plus carefully chosen electron optical viewing conditions (46).

3.3 Differential scanning calorimetry

Differential scanning calorimetry (DSC) is specifically designed method to measure the thermal properties of the material under examination (enthalpy or entropy changes etc.), whereas others simply monitor a property that changes with temperature and may produce data that are used directly without reference to the underlining thermal physics (46).

The structure of power-compensation type DSC instrument is shown in Fig. 3.2. The base of the sample holder assembly is placed in a reservoir of coolant. The sample and reference holders are individually equipped with a resistance sensor, which measures the temperature of the base of the holder, and a resistance heater. If a temperature difference is detected between the sample and reference, due to a phase change in the sample, energy is supplied until the temperature difference is less than a threshold value, typically < 0.01 K. The energy input per unit is proportional to the heat capacity of the sample. The maximum sensitivity of this instrument is 35 μW (49).

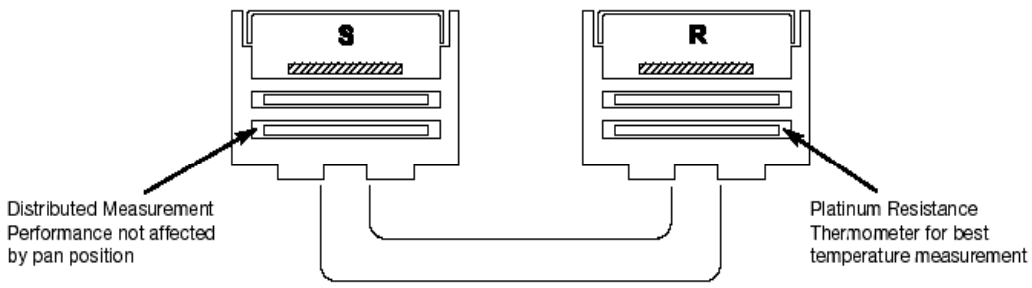

Fig. 3.2. Scheme of DSC instrument (50).

The temperature range of a power-compensation DSC system is between 110 and 1000 K depending on the model of sample holder assembly chosen. Some units are only designed to operate above 250 K, whereas others can be used over the entire temperature range. The heater of power-compensation DSC instrument is small so that the temperature response is quicker and higher scanning rates can be used. The maximum reliable scanning rate is 60 K/min. Isothermal experiments, annealing (single- and multi-step) and heat capacity measurements can be performed more readily using power-compensation type instrument (49).

3.4 Mechanical analysis

Plastics are polymeric materials and, to varying degrees, are non-linear viscoelastic. Consequently, their mechanical properties are functions of the ambient temperature, testing rate, magnitude of the excitation and other variables. This has strongly influenced the form and nature of the mechanical evaluation strategies and test procedures that have been adopted. Tests under conditions of constant rate of straining or stressing have been widely used for the mechanical evaluation of many classes of material long before they were adopted by the plastics community. For a viscoelastic material they constitute the class of ramp excitation tests (51).

3.4.1 Modulus from constant deformation rate

When applied to plastics, ramp excitation is primarily used to measure strength, for which it is eminently satisfactory. However, during the initial stages of the ramp it imposes an approximately constant straining rate on the specimen and with appropriate instrumentation short-term secant moduli and tangent moduli can be derived from the force–deformation curve, as displayed in Fig. 3.3. For plastics materials those moduli are multivalued because the force–deformation and stress–strain relations vary with the deformation rate and the ambient conditions and additionally are not linear (51).

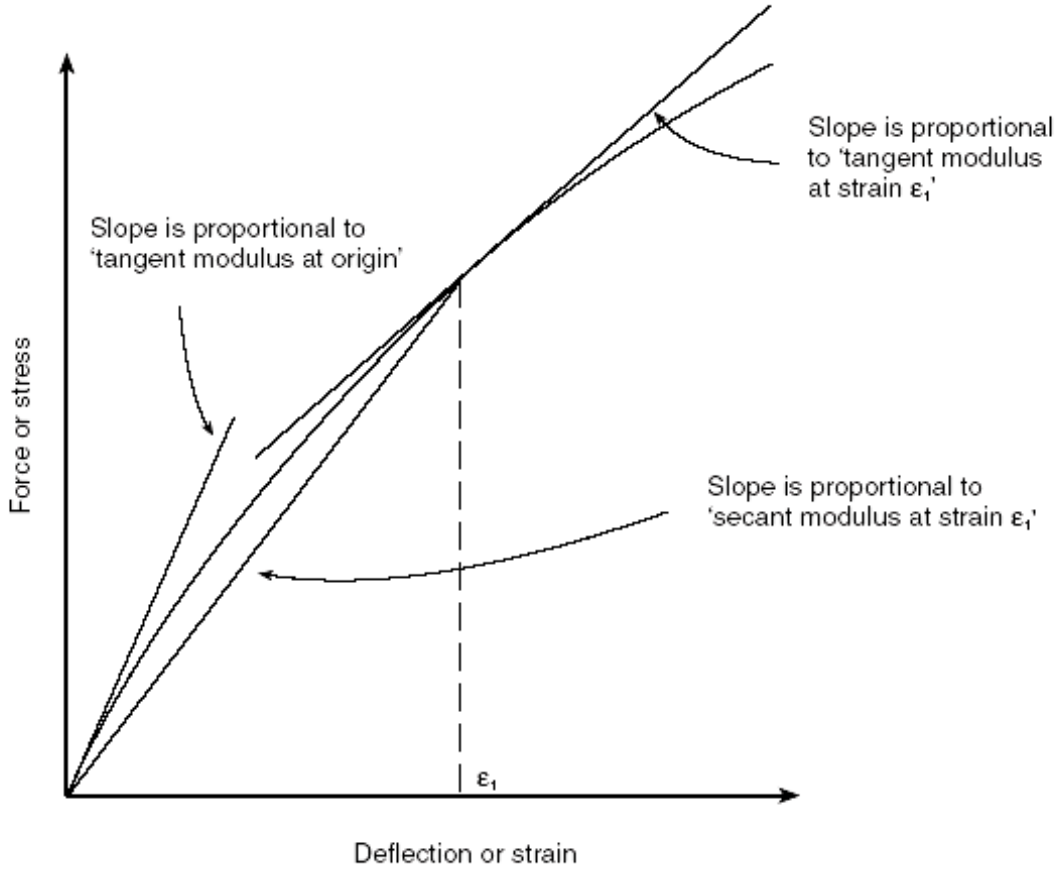

Fig. 3.3. Force-deformation relations below the yield point. The tensile modulus of most plastics materials decreases as the strain increases. The curvature is due to viscoelasticity and possibly structural change during the test (51).

"Modulus" relates to a material and translates into the stiffness of an article made from that material when the dimensions and load configuration are taken into account. For some classes of material, modulus can be regarded as a physical property the value of which should therefore be independent of the dimensions of the test specimen. However, this is not usually so for plastics because the properties vary with the degree of molecular order and other structural factors which, in turn, depend on the processing conditions and the flow geometry. Consequently, the stiffness of a plastics test specimen should be expressed only as the modulus of the material as manifest in that particular test piece (51).

The tensile modulus lies in the range 100 kPa to 1 MPa for a plastic in its rubbery state, in the range 2,5 GPa to 5 GPa for a plastic in its glassy state, and in the range 1 MPa to 1 GPa for amorphous plastics in their glass–rubber transition region and for crystalline plastics above their T_g (51).

3.5 Rheological measurements

Rheometry deal with quantitative measurements of flow properties of polymer melt and other systems, i.e. all characteristic values that determine their behaviour during flow. The steady state shear, dynamic linear viscoelastic shear, and elongational flows are most frequently used methods for description of polymer melts rheological properties. These can be classified according to strain (large for steady state shear vs. small for dynamic shear, moderate for extension flows), uniformity of stress, uniformity of strain rate, and different temperature and pressure conditions. The knowledge of rheological properties can be consequently employed for successful solution of many processing problems, such as the instability phenomenon (melt fracture) during the extrusion.

3.5.1 Shear rheometry

Shear rheometers are the primary tool of the experimental rheologist. It is convenient to divide shear rheometers into two groups: based on drag flow, like Couette apparatus, in which shear is generated between moving and fixed solid surfaces, and based on a pressure-driven flow, in which shear is generated by a pressure difference over a closed channel (52).

In the case of the pressure-driven apparatuses, the corrected shear viscosity as a function of corrected shear rate is counted by following procedure:

Firstly, corrected value of shear stress need to be evaluated by the help of the Bagley correction:

$$\tau = \frac{\left(P_L - P_0\right)}{2L_L} \cdot R \tag{3.1}$$

where P_L is pressure drop measured with long capillary, P_0 with orifice capillary; L_L represents long capillary length and R capillary radius. Then, apparent shear rate $\dot{\gamma}_a$ is determined from volume flow rate Q and capillary radius:

$$\dot{\gamma}_a = \frac{4Q}{\pi R^3} \tag{3.2}$$

Consequently, to obtain the true value of shear rate, Rabinowitch correction has to be applied:

$$\dot{\gamma} = \frac{4Q}{\pi R^3}\frac{3n+1}{4n} \tag{3.3}$$

where power-law index n is equal to quotient of $d(\log\tau)$ and $d(\log\dot{\gamma}_a)$. And finally, corrected shear viscosity could be calculated as:

$$\eta = \frac{\tau}{\dot{\gamma}} \tag{3.4}$$

3.5.2 Elongational rheometry

Measurement of elongational viscosity is accompanied with several problems. Many different methods have been used to solve these problems and generate purely elongational flow. The most successful geometries can be divided into two groups. The first – simple extension, compression, and sheet stretching, are methods suitable for solids, particularly for rubber (53). They can all give homogenous, purely elongational deformations, but because their success depends on holding onto the edges of sample, they have only been used successfully with higher viscosity samples. The second group represents attempts to elongational functions measurement for lower viscosity liquids. The most significant members of this group are: fibre spinning, bubble collapse, stagnation flows and entrance flow (52). Measurement based on entrance flow is paid attention in following few paragraphs.

As the fluid flows from a large cross section tube (reservoir) into a small cross section tube (capillary), the streamlines converge. To overcome this reduction in the cross-sectional area and continue to flow, the fluid dissipates extra energy, which is expressed as the entrance pressure drop. The converging streamlines indicate the elongational flow.

To simplify the calculation of the elongational viscosity from entrance pressure drop measurements, several approximate analyses have been proposed. The most significant according to (54) are: sink flow analysis by Metzner and Metzner (55), Cogswell analysis (56) and two methods by Binding (57-59).

In present work, Cogswell (56) method, assuming contributions from both shear and elongational components of flow in the contraction region, is employed. The shear viscosity is assumed to obey power-law, while the elongational viscosity is supposed to be constant (54). In converging region, both these contributions benefit to the total pressure drop. Converging flow at an orifice capillary may be approximated by saying that the melt

flows through an infinite set of very short cylindrical dies (56). The overall pressure drop used for determination of elongational data is then calculated by minimising an infinite sum of the elemental pressure drops along elements (52).

Cogswell method in mathematical point of view could be described as follows:

While, elongational stress σ_e is given by equation:

$$\sigma_e = \frac{3}{8}(n+1)P_0 \tag{3.5}$$

elongational viscosity η_e is defined as:

$$\eta_e = \frac{9}{32}\frac{(n+1)^2}{\eta}\left(\frac{P_0}{\dot{\gamma}}\right)^2 \tag{3.6}$$

Finally, elongational rate $\dot{\varepsilon}$ is simply:

$$\dot{\varepsilon} = \frac{\sigma_e}{\eta_e} \tag{3.7}$$

3.5.3 Rheology of multiphase systems

In the case of polymer blends, there are many interrelated variables that affect their rheological behaviour, processability, and mechanical-physical properties of the final product. For instance, the blend preparation (e.g. the method of mixing the polymers and intensity of mixing) determines the morphology of the blend (i.e. size of the dispersed phase, and the dispersed phase size distribution), which consequently controls rheological properties of the blend. In other words, it is noteworthy that the rheological behaviour strongly dictates the choice of processing conditions. In multiphase systems the large and the small strain measurements lead to distinctly different structures. In contrast to rheometry of homogeneous, single-phase liquids, here the selection of the deformation mode provides different responses. These facts in turn significantly influence the morphology and, therefore, the overall properties of the finished product (60).

In order to understand complex rheological behaviour of polymer blends, well-known systems are used as the models. To approximate miscible polymer blends, mixtures of low molecular weight liquids (i.e. solutions), or blends of polymeric fractions (homologous polymer blends) can be employed. For various types of immiscible systems, suspensions can serve as models for blends with low concentration of more viscous polymer, emulsions

as a general model of blends with dispersed morphology, and block copolymers for well-compatibilised blends and/or polymer blends with co-continuous morphology.

From the rheological point of view, polymer blends can be classified by the relation between their melt viscosity and composition with respect to the log-additivity rule

$$\log \eta = \sum_i w_i . \log \eta_i \qquad (3.8)$$

where w_i and η_i denote, respectively, the weight (or volume) fraction and viscosity of ingredient "i" in the blend. Thus, polymer blends can be divided as: additive ones (which follow Eq. 3), blends showing a positive deviation from the log-additivity, blends with a negative deviation, and blends with both positive and negative deviations (61).

In principle, the viscosities in Eq. 3 should be taken at zero deformation rates. However, this is not possible to be determined for a number of polymeric systems. In such a case, the viscosity at a constant level of stress should be used. As recommended in several sources (1, 62, 63), this approach is more reasonable than using viscosity at constant deformation rate, since in the absence of interfacial slip the stresses are continuous across the interphase, while the deformation rates are not (1, 17).

The classification of polymer blends based on the viscosity versus composition dependence does not necessarily characterize the polymer pair, but rather the mechanism of the flow prevalent under the testing conditions. Changing the molecular weight or testing temperature may significantly alter the flow mechanism, and consequently the type of deviation from the log-additivity rule. To conclude, due to the diversity of morphology and rheological responses observed for immiscible blends, any attempt to generalize must be viewed with suspicion (1).

4 EXPERIMENTAL PART

In this chapter, the attention is paid to description of used materials, preparation of blends, specimen processing and analyses of structure and properties.

4.1 Preparation of blends

Linear high-density polyethylene LITEN TB 38 and isotactic polypropylene MOSTEN GB 003, both produced by Chemopetrol Litvínov, Czech Republic, were chosen as starting materials in this study. Both materials are common-available polymers employed in consumer industry. Selected characteristics of these materials provided by producer are shown in Table IV.1.

Table IV.1. Characteristics of PP MOSTEN GB 003 and PE LITEN TB 38.

Property	Unit	Typical merit		Testing method
		PE	PP	
Melt-flow index	g/10 min	0.55 (190/2.16)	3.20 (230/2.16)	ISO 1133
Density	kg/m^3	954	907	ISO 1183
Yield stress	MPa	25	34	ISO 527
Flexural modulus	MPa	1250	1600	ISO 178

PP/PE blends were prepared using counter-rotating twin-screw extruder at screw speed 35 rpm. The temperature of extruder ranged from 190 °C (in the melting zone) to 210 °C (in the metering zone and the die). The extruded filaments of blends with 20, 30 and 40 wt.% of PP were quenched and granulated.

4.2 Direct extrusion of MFC

One of the ways to prepare blend of incompatible polymer pair in which the dispersed phase forms in-situ reinforced fibres is utilisation of extrusion line equipped with conical-convergent die. Hence, in the present study, a die of this type was employed for extrusion of MFC tapes in one processing step.

The whole extrusion line consisted of:

- A Brabender measuring single-screw extruder 30/25 D (Brabender OHG Duisburg, Germany);
- a Zenith PEP II gear pump 1.2 cm^3/rev (Zenith Pumps, Sanford, NC, USA) which enabled up to 25 MPa pressure increase and produced uniform flow of the melt;

- a flat extrusion die with 2x20 mm outlet cross-section. The polymer melt passing through die was firstly accelerated in convergent section with semi-hyperbolic convergency and subsequently cooled in calibration section.

Final extrusion rate was governed by revolutions of gear pump that were either 20 or 30 rpm. The temperature profile within the extrusion line was carefully controlled. While temperatures of extruder and gear pump, T_1-T_4 and T_{pump}, were constant throughout the experiment (150, 170, 190, 210 and 200 °C, respectively), temperatures of the die sections varied as shown in Table IV.2. In this way, extrudates with different processing history were obtained which enabled to assess the impact of processing on structure and properties of MFC blends.

Table IV.2. Summary of processing conditions where cyl stands for cylinder zone, con is converging zone, and cal means calibration zone.

Mode	T_{cyl} (°C)	T_{con} (°C)	T_{cal} (°C)	Gear pump (rev/min)
1	195	190	180	20
2	185	170	170	20
3	185	170	170	30
4	185	165	170	20
5	185	165	170	30

In addition, for determination of the effects of compounding on resulting morphology and properties of MFC products, extrudates were prepared from both compounded blends and hand-mixed polymers (time of mixing was approximately 3 min), at each above-mentioned extrusion mode.

The prepared specimens were labelled by 4 characters indicating the content of PP in blend (20, 30 and 40), compounding process (c – compounded, n – hand-mixed) and extrusion mode (1-5). For example:

- 20c1 labelled specimen was extruded under mode 1 from the compounded blend with 20 wt.% of PP.
- 30n5 labelled specimen was extruded under mode 5 from the hand-mixed blend with 30 wt.% of PP.

4.3 Analyses of structure and properties

Structure and properties of polymer parts are mutually interconnected. Hence only description of specimen properties combined with results of structure analyses can provide comprehensive understanding of investigated systems.

4.3.1 Wide-angle X-ray diffraction

Wide-angle X-ray scattering was applied to determine crystallinity and degree of orientation of the specimens. Experiments were performed in transmission mode with HZG diffractometer. Radial scans of intensity vs. diffraction angle 2θ were recorded in the range of 10-30º by steps of 0.05º and step scan interval of 5 s at ambient temperature. Specimens with dimension of 100x20x2 mm were prepared from all sets of extrudates and irradiated perpendicular and parallel to extrusion direction. Crystallinity (X_C) of the extrudates was evaluated as the ratio of the integral intensities diffracted by a crystalline part I_C and total integral intensities I:

$$X_C = \left(\frac{I_C}{I} \right) \cdot 100 \qquad (4.1)$$

4.3.2 Electron microscopy

Structure of extrudates was examined using a Jeol JSM-35 scanning electron microscope and an EM Tesla BM 500 transmission electron microscope. For scanning electron microscopy, the extrudates were broken in liquid nitrogen and, subsequently, the crack surfaces were coated by a thin gold layer and observed. For transmission electron microscopy, the polyvinylalcohol-replicas of the surfaces etched for 10 min in 1% solution of $KMnO_4$ in 85% H_3PO_4 were used.

4.3.3 Differential scanning calorimetry

A power-compensation differential scanning calorimeter (DSC Pyris 1 Perkin-Elmer Co., USA) was employed for the investigation of thermal behaviour of extrudates. Thin cross-sectional cuts (approx. 120 μm thick) were microtomed using a FOK GYEM OE-908 microtome from extruded tapes and loaded into aluminium pans. Then, the samples were heated from 50 °C up to 190 °C at heating rate of 10 °C/min. Nitrogen as a pure gas was

used and constantly passed (20 ml/s) through heat sink and over the cells. From resulting thermograms, melting temperature and heat of fusion were calculated.

4.3.4 Tensile test

Tensile properties of extruded MFC tapes were tested by means of an Instrone 8871 tensile testing machine at ambient temperature. Specimens with gauge length of 30 mm, width of approx. 3 mm and thickness of approx. 2 mm were strained at initial rate of 1 mm/min to 1% strain for accurate E-modulus determination. Then, the testing continued at the strain rate of 100 mm/min.

4.3.5 Rheological measurement

Rheological measurements were carried out using RH7-2 capillary rheometer (Rosand Precision, Ltd., England). This is a twin bore instrument providing two simultaneous measurements with short (orifice) and long capillaries. The experiments were performed at temperature of 180 °C in a constant piston speed mode at shear rate range approx. from 10^1 to 10^4 s^{-1}. Bagley and Rabinowitch correction and Cogswell method were applied automatically on the measured data by Rosand rheometer software.

The dimensions of the capillaries and barrels were:

- short (orifice) capillary: $L_0 = 0$ mm, $D_0 = 1$ mm
- long capillary: $L_L = 16$ mm, $D_L = 1$ mm
- barrel: $D_B = 15$ mm

5 RESULTS AND DISCUSSION

Extrudates prepared from polymer blends as well as from pure components were compared by structure analyses and thermal, mechanical and rheological measurements in order to determine optimal blend composition and processing mode of extrusion. Details of results and their discussion are presented in following chapters.

5.1 Structural analyses

5.1.1 X-Ray scattering

X-Ray scattering was employed to determine two important characteristics of extrudates, namely crystallinity and degree of PP orientation in the blends.

Although X-Ray method can be easily employed for evaluation of crystallinity of pure polymers, it cannot be simply utilized for crystallinity assessment of individual phases in polymer blends because some reflections are mutually overlapped (see Fig. 5.1). Thus, obtained crystallinity of polymer blends has only a low predicative value, and it is not given here. Calculated crystallinity levels of pure PE and PP are listed in the following Table V.1. As can be seen, the crystallinity ranges between 0.50 and 0.55 for PP and 0.58 and 0.62 for PE extrudates. However, the values in both materials are not significantly affected by varying processing conditions. This low sensitivity of PP and PE to processing set-up is caused by their high crystallizability and method used. It is predictable that the skin layer of extrudates is particularly affected by channel temperature and shear stresses arising in flowing melt. Nevertheless, wide-angle X-ray scattering in transmission mode provides an integral value of crystallinity and therefore cannot reflect the changes within profile.

Table V.1. Crystallinity of extrudates from pure materials at different processing conditions.

Mode	Crystallinity of PP	Crystallinity of PE
1	0.52	0.60
2	0.51	0.58
3	0.53	0.60
4	0.55	0.60
5	0.50	0.62

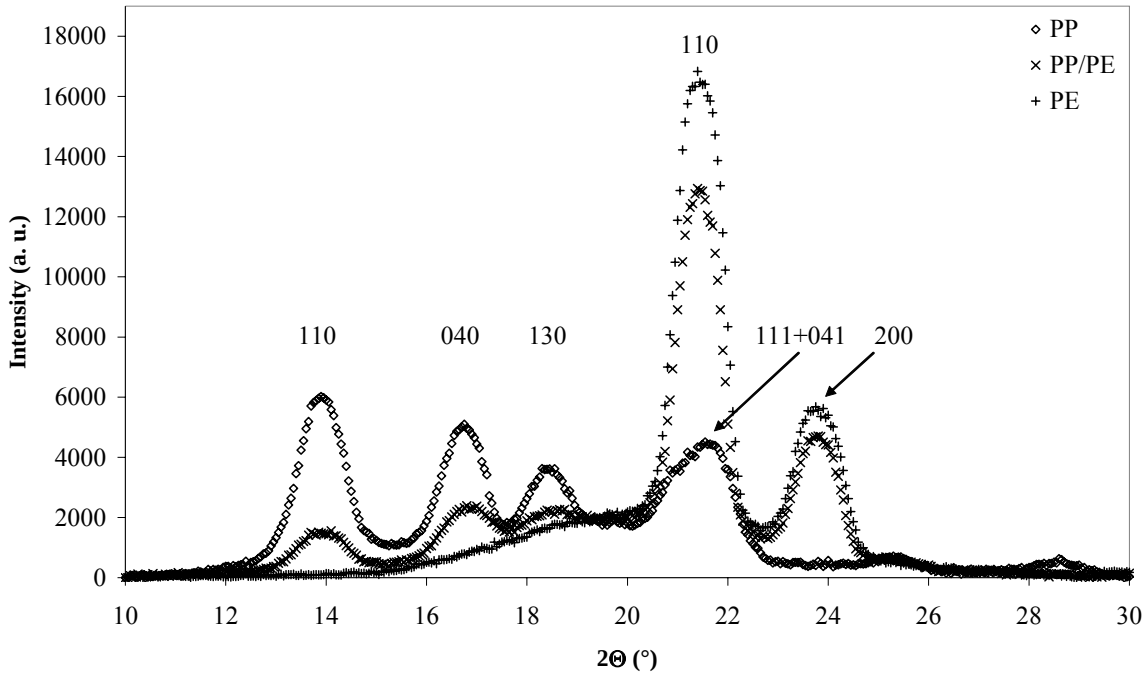

Fig. 5.1. X-Ray records of PP, PE and PP/PE blend.

The level of orientation in reinforcing PP phase is an important parameter which should be taken into account for the explanation of mechanical properties of prepared PP/PE blends. Trotignon et al. (64) suggested the evaluation of crystalline orientation in PP (*A*) as a ratio between the intensities of (110) and (111+041) reflections:

$$A = \frac{I_{(110)}}{I_{(110)} + I_{(111+041)}} \tag{5.1}$$

Unfortunately, the equation cannot be used in PP/PE blends because PP (111+041) reflection is overlapped by PE (110) reflection (see Fig. 5.1). Thus, in this work, different relation based on the changes in intensities of (110) and (040) reflections with rising degree of orientation was suggested. As can be seen in Fig. 5.2 the intensity of (040) reflection decreases with degree of orientation while the intensity of (110) reflection is intensified. Consequently, degree of orientation (*O*) can be evaluated as:

$$O = \frac{I_{(110)}}{I_{(110)} + I_{(040)}} \tag{5.2}$$

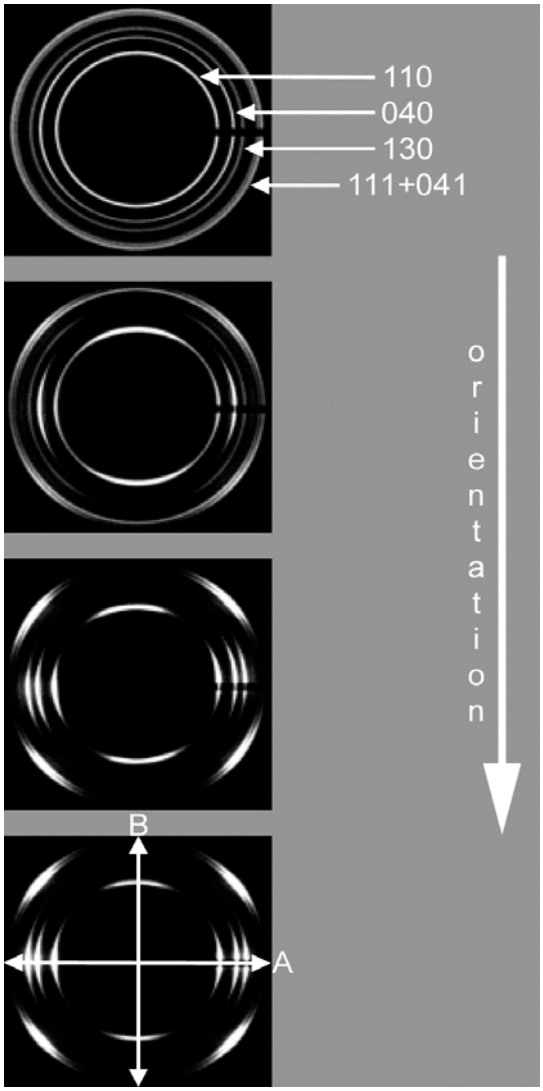

Fig. 5.2. X-ray patterns of polypropylenes with varying degrees of orientation.

Figs. 5.3 and 5.4 display orientation of PP in extruded tapes as a function of PP content. Generally, the orientation in blends is higher compared to pure PP extrudates and it increases with rising amount of PP. However, from comparison of the Figs. 5.3 and 5.4 is evident that the impact of processing conditions, i.e. changes in the modes, is more pronounced in hand-mixed blends. This result indicates that the size and shape of PP domains in these blends is more transformed during the extrusion, compared to the compounded blends, in which the orientation is rather insensitive to processing set-up used.

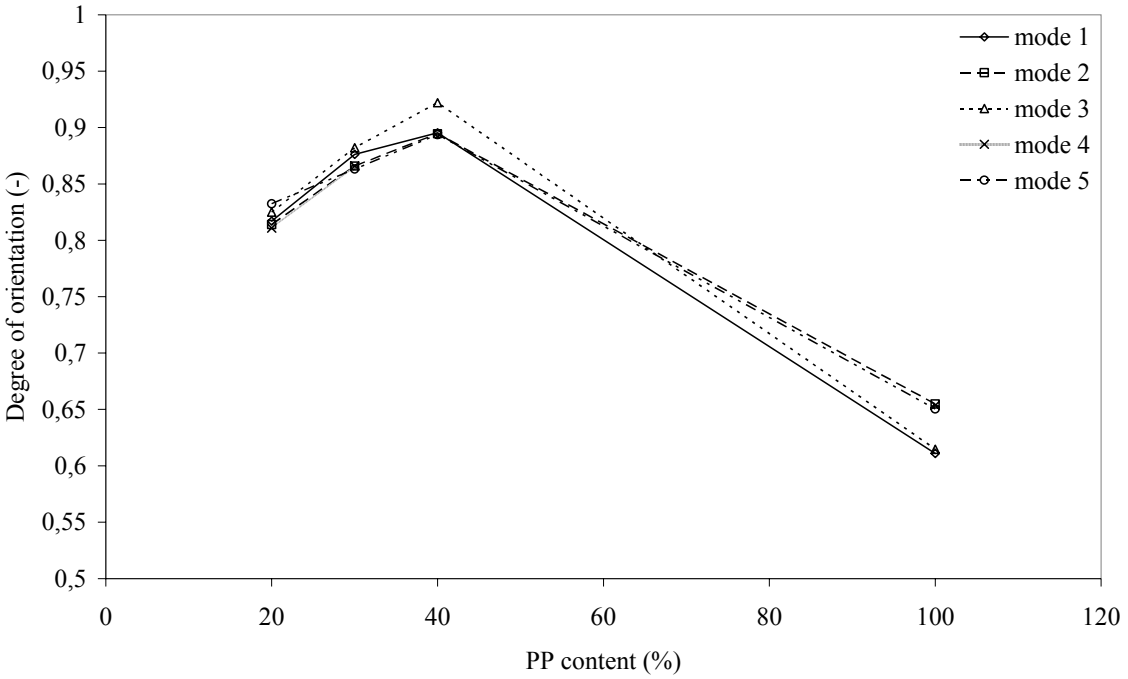

Fig. 5.3. Degree of orientation in extrudates from compounded blends as a function of blend composition.

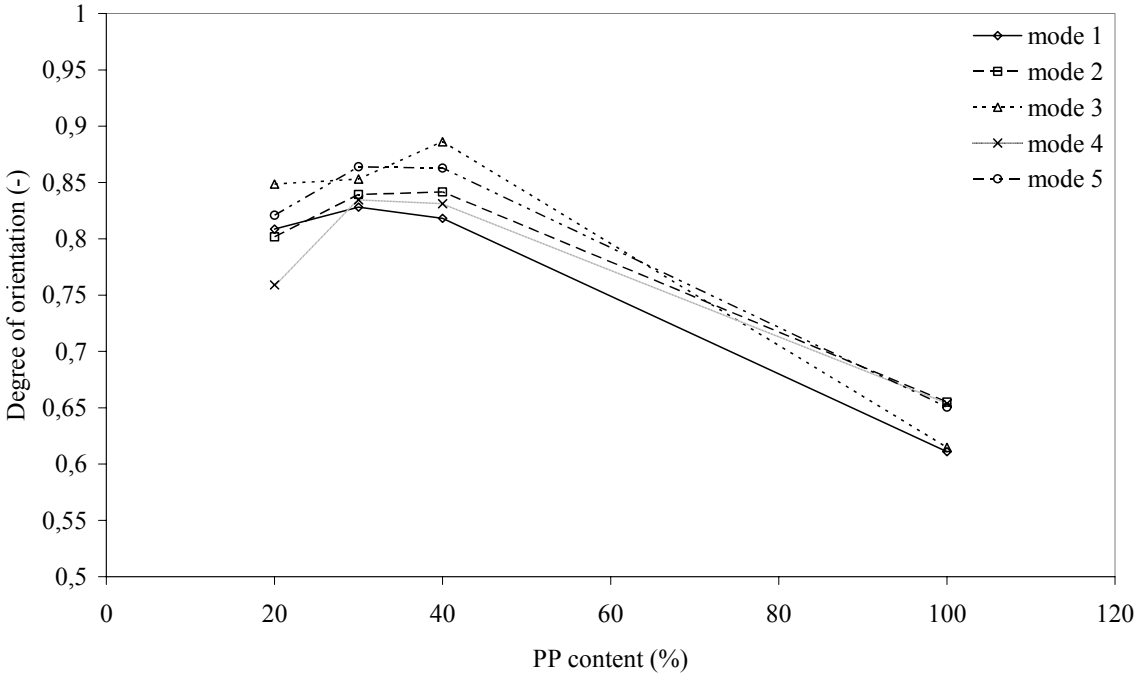

Fig. 5.4. Degree of orientation in extrudates from hand-mixed blends as a function of blend composition.

5.1.2 Electron microscopy

Structure of crack surfaces of extruded tapes was examined by scanning electron microscopy (SEM). The scanned micrographs can be seen in Figs 5.5-5.9. While the micrographs of pure extrudates show isotropic structure, the morphology of the tapes extruded from blends is oriented along the flow direction. This is important result and the first prerequisite to rate these blends as microfibrillar-phase composites. As can be seen from comparison of Figs. 5.5-5.9 the structure of compounded-blend extrudates gradually changes from fine-fibril morphology to coarse co-continuous phase structure, in respect of the PP content increase. On the other hand, this structure gradation is not clearly shown in the extrudates prepared from hand-mixed materials. Although the transition between fibrillar and co-continuous morphology can be recognized, the diameter of PP domains is not directly controlled by the PP content; similarly to results from wide-angle X-ray scattering, the diameter of the PP domains in extrudates from hand-mixed materials seems to be rather influenced by the processing condition than the blend composition.

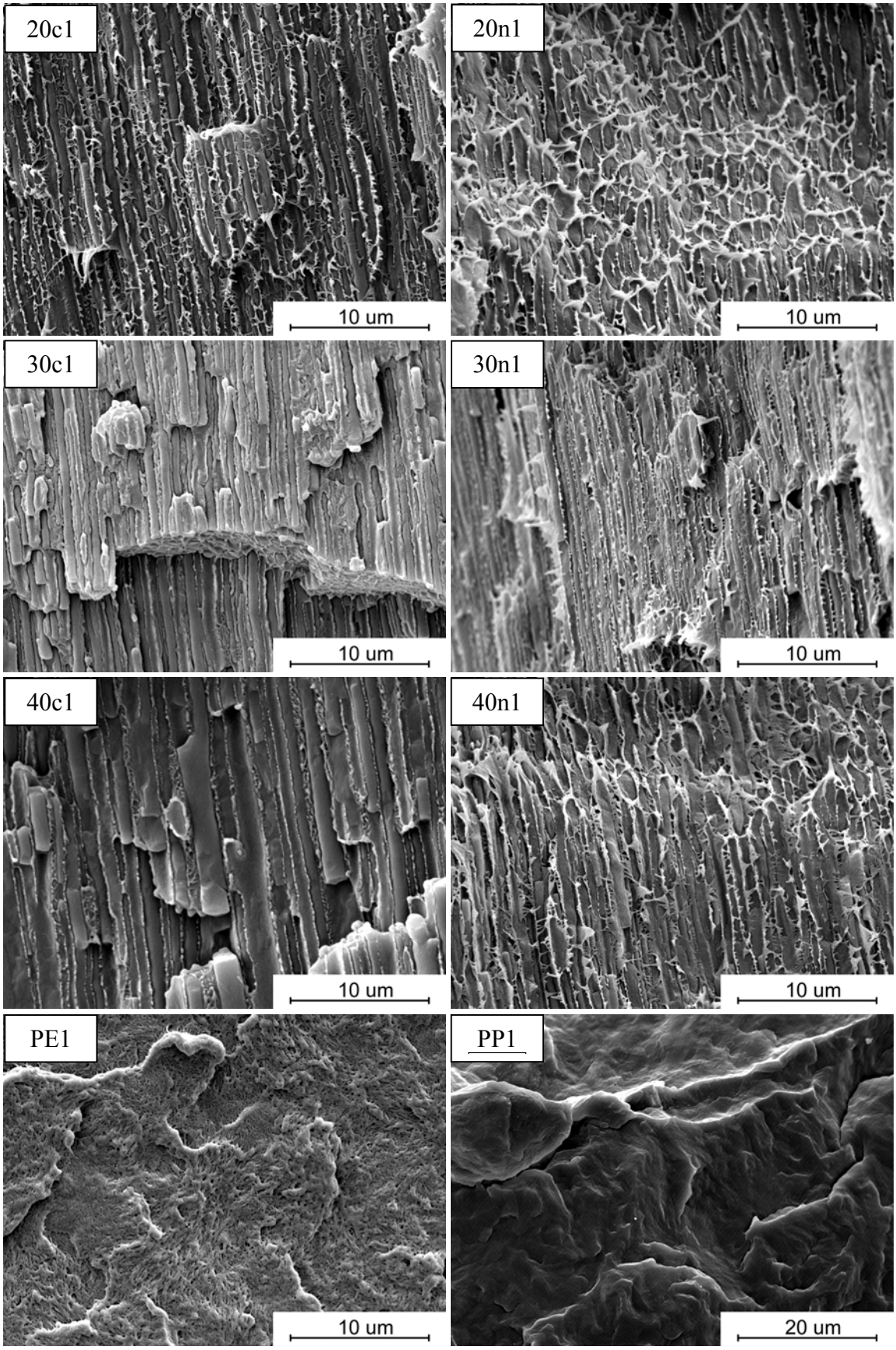

Fig. 5.5. SEM micrographs of extrudate morphology originated via extrusion mode 1.

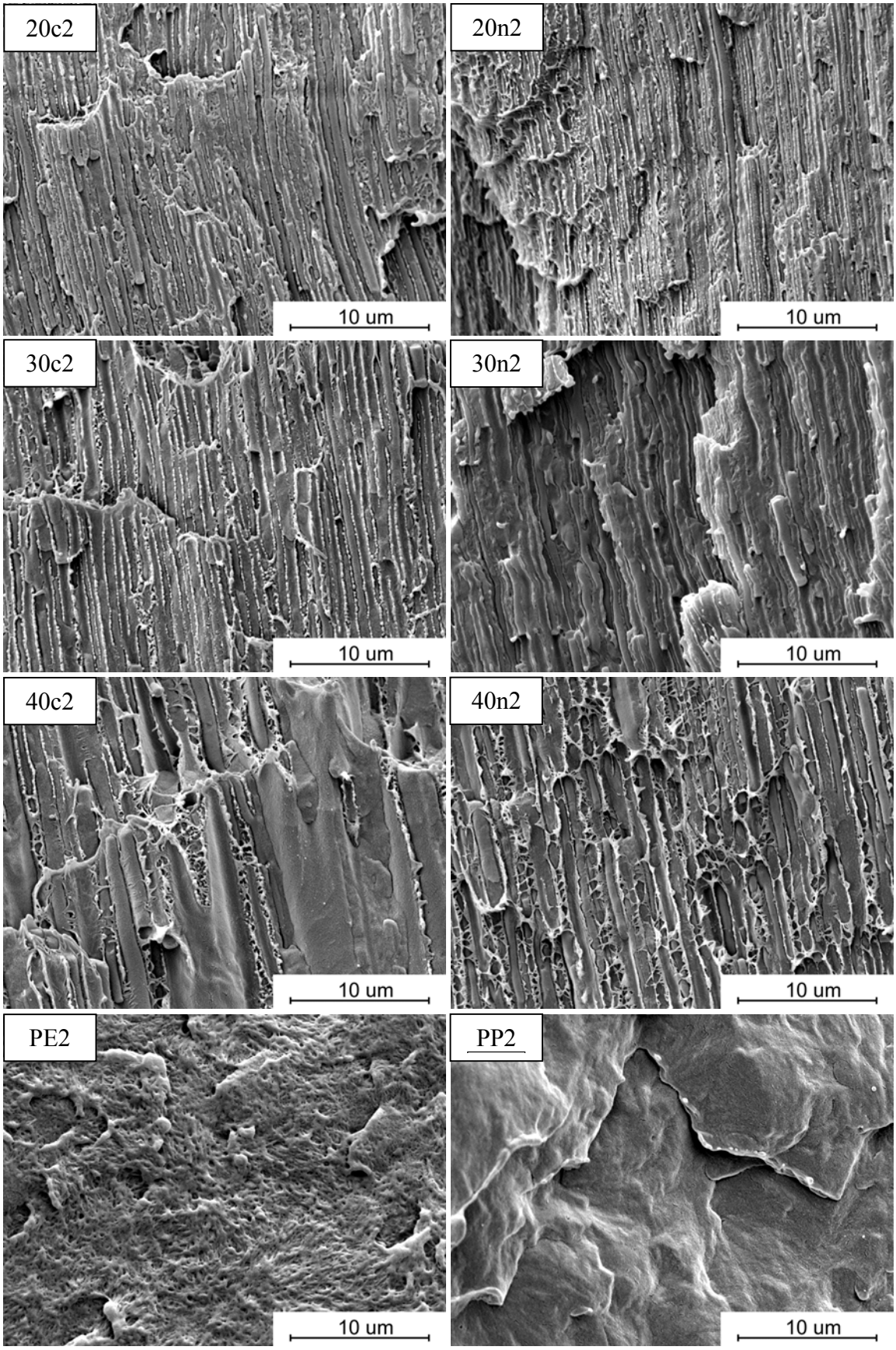

Fig. 5.6. SEM micrographs of extrudate morphology originated via extrusion mode 2.

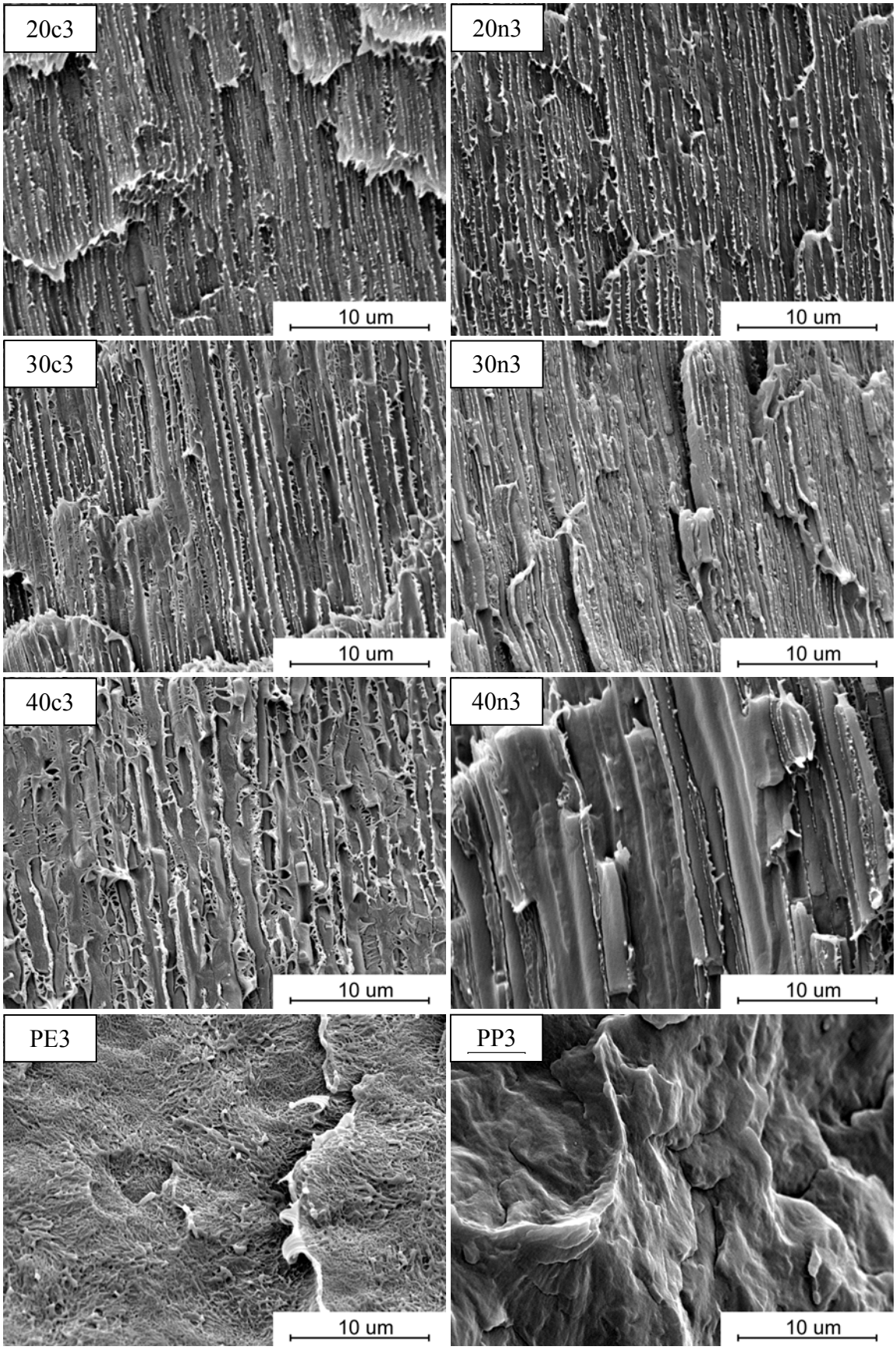

Fig. 5.7. SEM micrographs of extrudate morphology originated via extrusion mode 3.

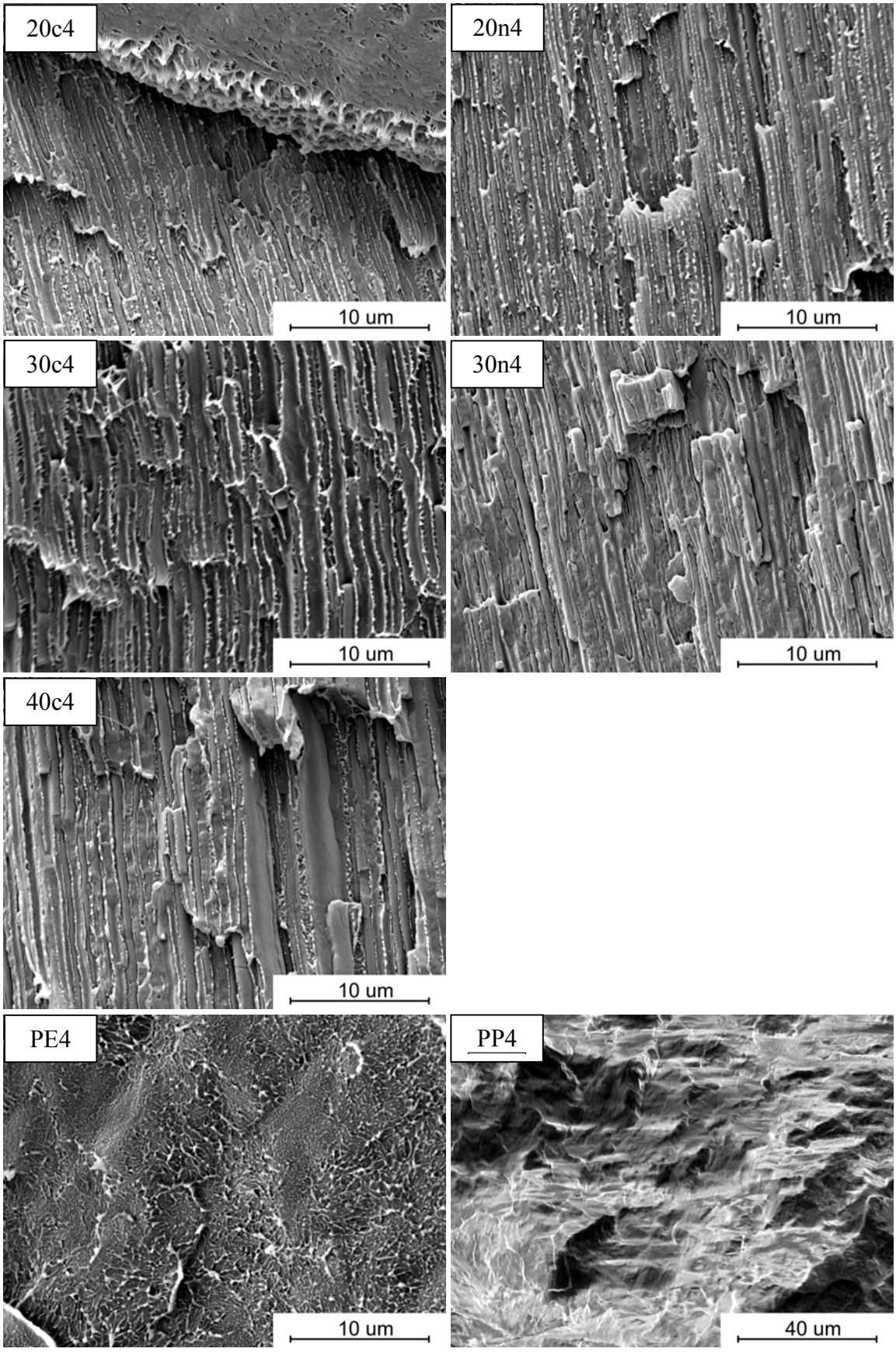

Fig. 5.8. SEM micrographs of extrudate morphology originated via extrusion mode 4.

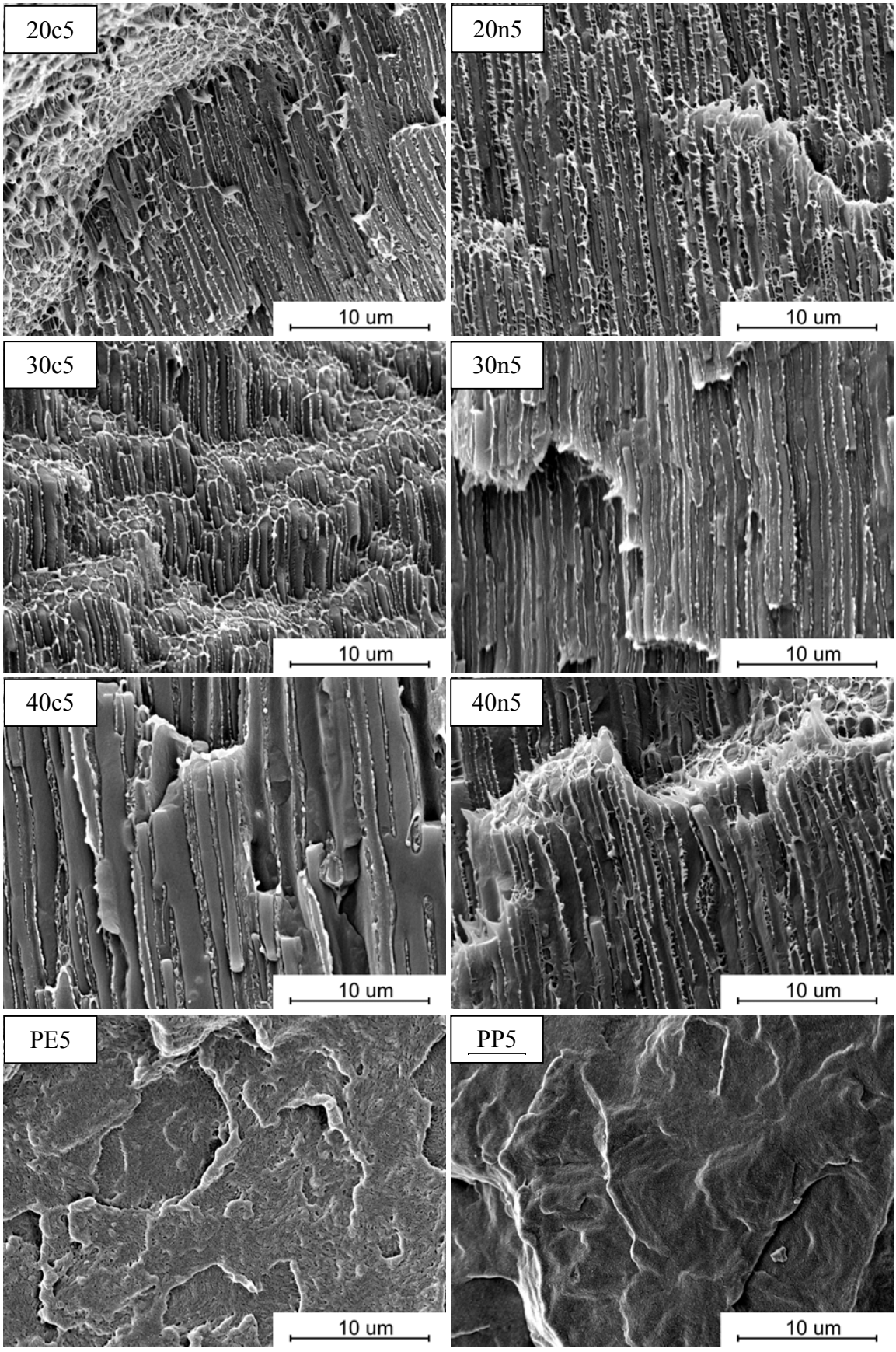

Fig. 5.9. SEM micrographs of extrudate morphology originated via extrusion mode 5.

Details of the surface morphology of extrudates were taken by transmission electron microscopy (TEM). In this work, the set of micrographs taken form the tapes prepared at mode 5 is presented in Fig. 5.10. In the micrographs of PE extrudate, an isotropic lamellae structure can be found. On the other hand, the surface of PP tape shows oriented lamellae structure. This discrepancy between PE and PP morphology can be explained by the differences in the level of shear stresses arising during the flow near the surface. As the melting/crystallization temperature of PP is shifted to higher values, in fact, this material was processed at more severe conditions manifesting itself in the higher level of surface orientation, compared to that of PE. It can be also recognized that the lamellae of PP are several-folds finer. Due to this difference in PE/PP lamellae dimensions, the individual materials can be simply recognized even in the blends. It is evident that the morphology of the blends consists of varying amount of PP oriented-lamellar fibrils and PE epitaxial-crystallized lamellae on the PP fibrils at the angle of approx. 50 °. This fact was described in several works and discussed in theoretical background of present work.

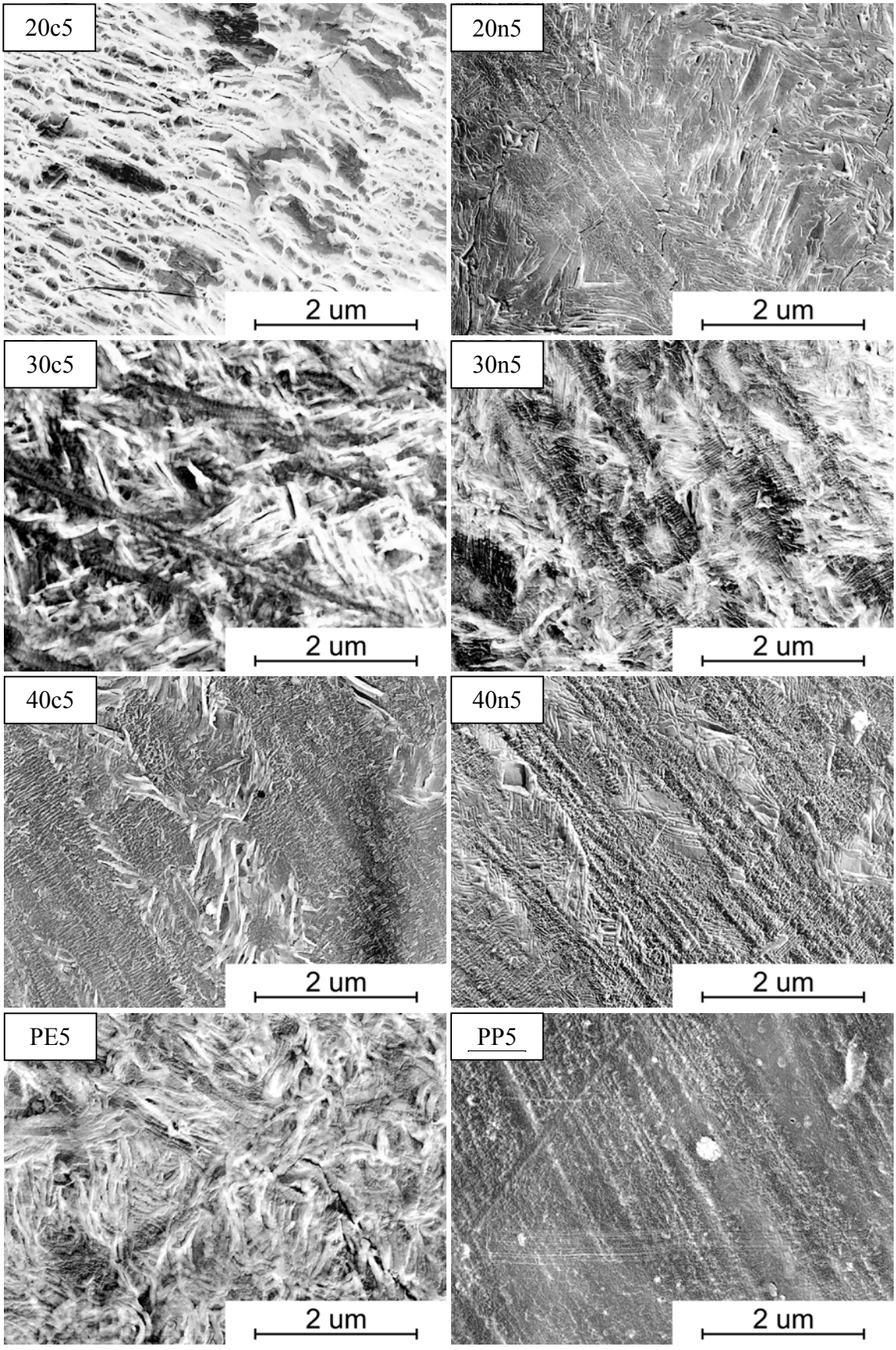

Fig. 5.10. TEM details of extrudate morphology originated during extrusion mode 5.

5.1.3 DSC analysis

The DSC analysis was employed to examine thermal behaviour of extruded tapes. From Figs. 5.11-5.15 can be seen that the shapes and intensities of the melting peaks varies with the composition of the blends. In comparison with the thermal scans of hand-mixed blend extrudates, the melting peaks of individual phases in compounded blends are slightly shifted towards themselves. This fact indicates a limited miscibility at interfaces and subsequent co-crystallization occurring in these blends during extrusion. Consequently, this co-crystallization of both components can increase dramatically interface cohesion which can results in improvement of mechanical properties.

Tables V.2-V.6 display calculated values of melting temperatures and heats of fusion of extrudates. As can be seen the heats of fusion of PP and PE components in compounded blends show slightly higher values than those of hand mixed blends, which reflects generally higher level of macromolecular order resulting from enhanced phase mixing upon twin-screw blending. Nevertheless, the effect of processing conditions on thermal behaviour of all the extrudates is diminutive as manifested by nearly identical values of melting temperature and heat of fusion.

Table V.2. Melting temperatures and heats of fusion of extrudates prepared at mode 1.

%PP	Compounded blends				Hand-mixed blends			
	PE		PP		PE		PP	
	T_m	ΔH	T_m	ΔH	T_m	ΔH	T_m	ΔH
0	-	-	-	-	130.3	193.0	-	-
20	130.4	152.4	162.5	17.9	128.9	140.7	163.2	16.7
30	129.9	130.5	162.5	23.8	129.1	120.1	163.0	26.0
40	130.3	109.8	162.5	33.8	129.1	104.9	162.5	36.1
100	-	-	-	-	-	-	165.3	89.8

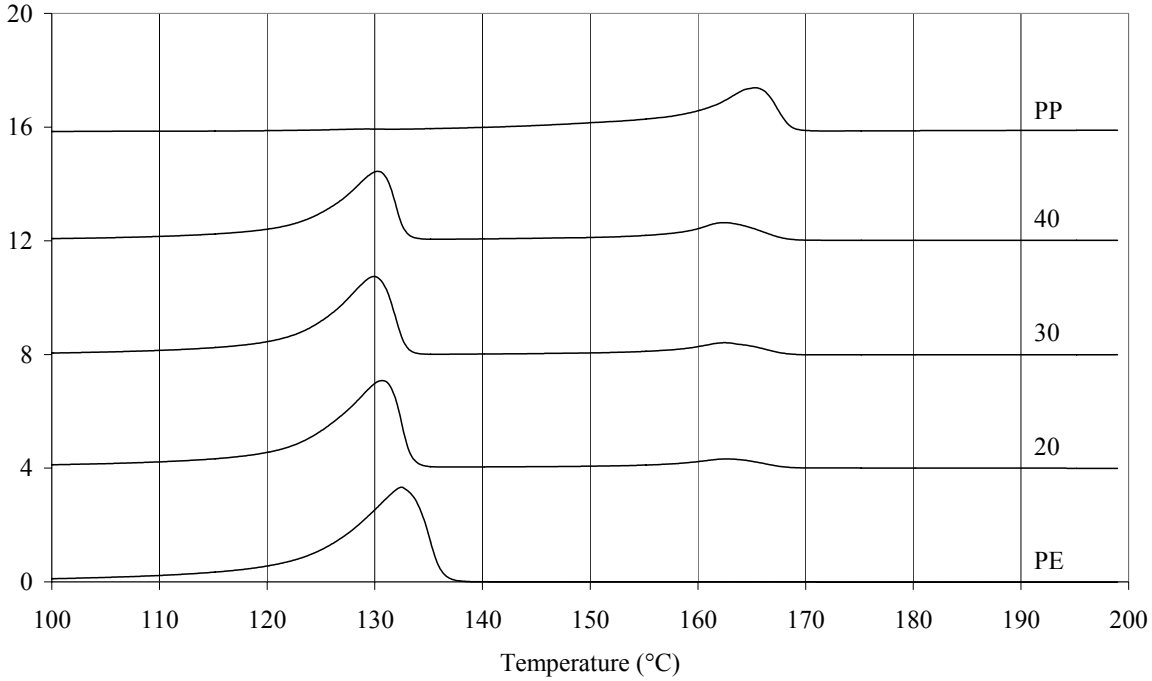

Fig. 5.11. Thermal scans of tapes extruded at mode 1 from pure and blended polymers. Solid line represents samples prepared from compounded blends and dashed line is used for hand-mixed blends.

Table V.3. Melting temperatures and heats of fusion of extrudates prepared at mode 2.

%PP	Compounded blends				Hand-mixed blends			
	PE		PP		PE		PP	
	T_m	ΔH	T_m	ΔH	T_m	ΔH	T_m	ΔH
0	-	-	-	-	131.1	195.8	-	-
20	130.4	162.9	162.9	18.6	129.7	146.4	163.0	17.5
30	130.2	132.9	162.3	25.7	129.7	123.6	162.9	27.8
40	130.1	111.2	162.8	34.3	129.1	107.7	162.4	33.4
100	-	-	-	-	-	-	164.5	95.7

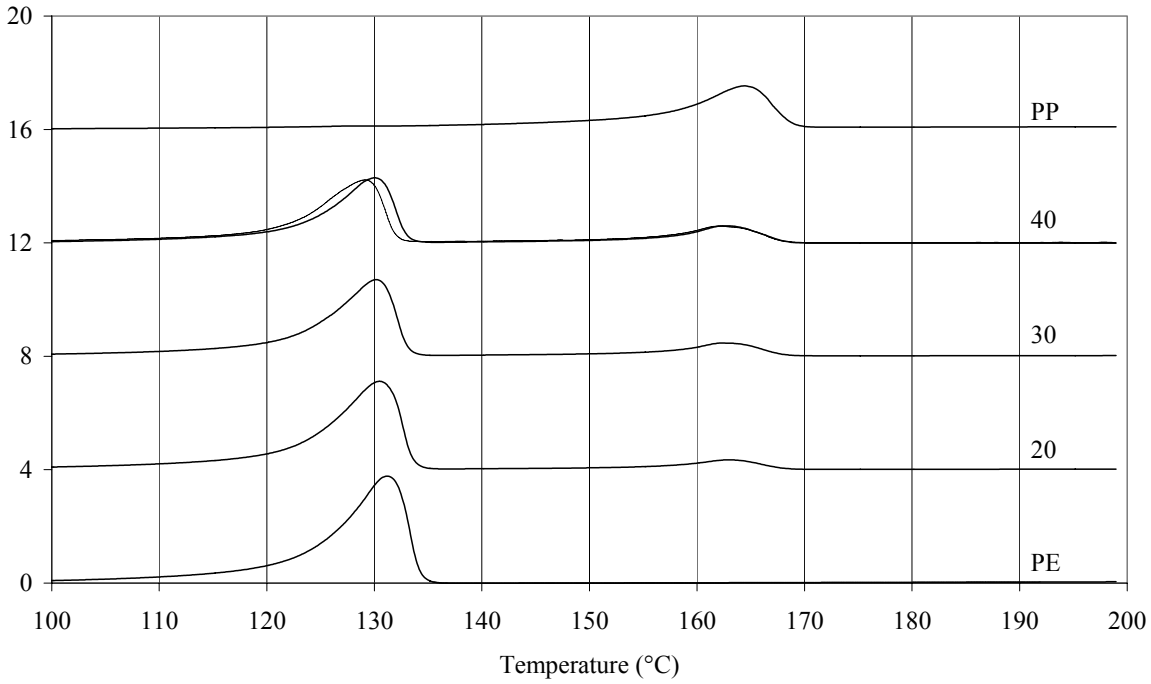

Fig. 5.12. Thermal scans of tapes extruded at mode 2 from pure and blended polymers. Solid line represents samples prepared from compounded blends and dashed line is used for hand-mixed blends.

Table V.4. Melting temperatures and heats of fusion of extrudates prepared at mode 3.

%PP	Compounded blends				Hand-mixed blends			
	PE		PP		PE		PP	
	T_m	ΔH	T_m	ΔH	T_m	ΔH	T_m	ΔH
0	-	-	-	-	130.3	190.6	-	-
20	130.1	145.6	162.7	16.6	129.4	143.5	163.2	17.1
30	130.6	132.1	162.6	25.6	130.2	132.5	163.0	26.2
40	130.4	114.7	163.0	34.9	129.9	109.3	163.0	34.7
100	-	-	-	-	-	-	164.5	101.4

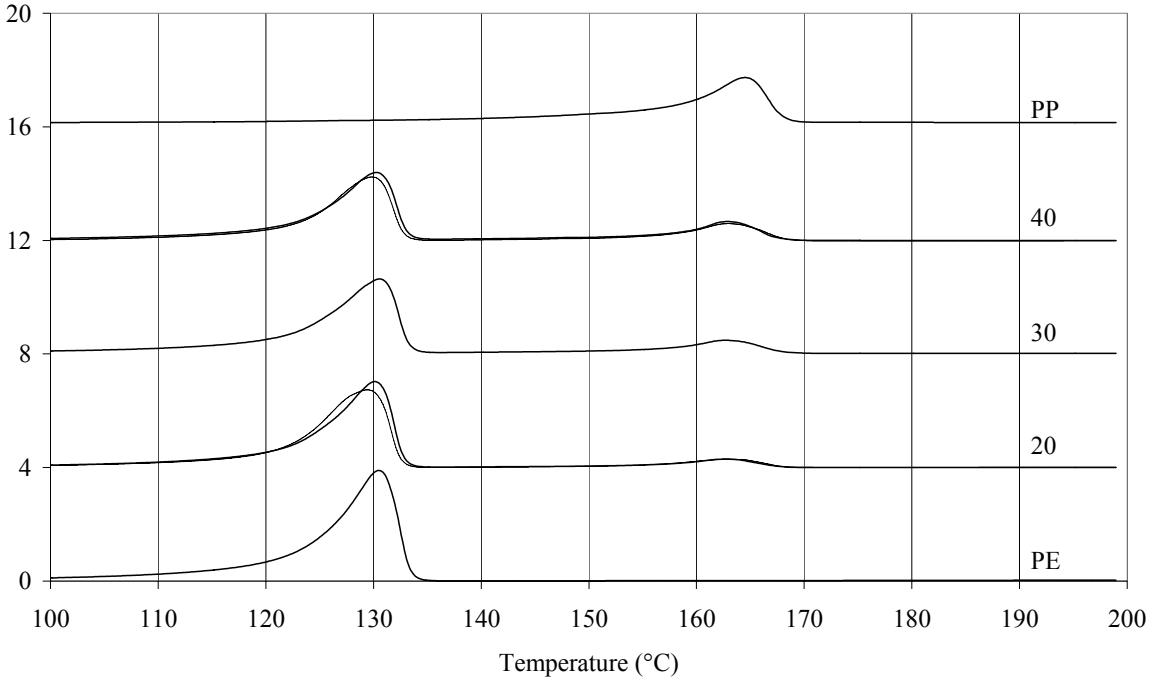

Fig. 5.13. Thermal scans of tapes extruded at mode 3 from pure and blended polymers. Solid line represents samples prepared from compounded blends and dashed line is used for hand-mixed blends.

Table V.5. Melting temperatures and heats of fusion of extrudates prepared at mode 4.

%PP	Compounded blends				Hand-mixed blends			
	PE		PP		PE		PP	
	T_m	ΔH	T_m	ΔH	T_m	ΔH	T_m	ΔH
0	-	-	-	-	130.5	192.6	-	-
20	130.1	144.4	162.0	15.7	129.4	144.0	163.0	17.2
30	130.2	132.1	162.8	25.3	130.3	125.3	163.7	26.6
40	-	-	-	-	129.4	104.2	162.8	36.4
100	-	-	-	-	-	-	164.9	100.4

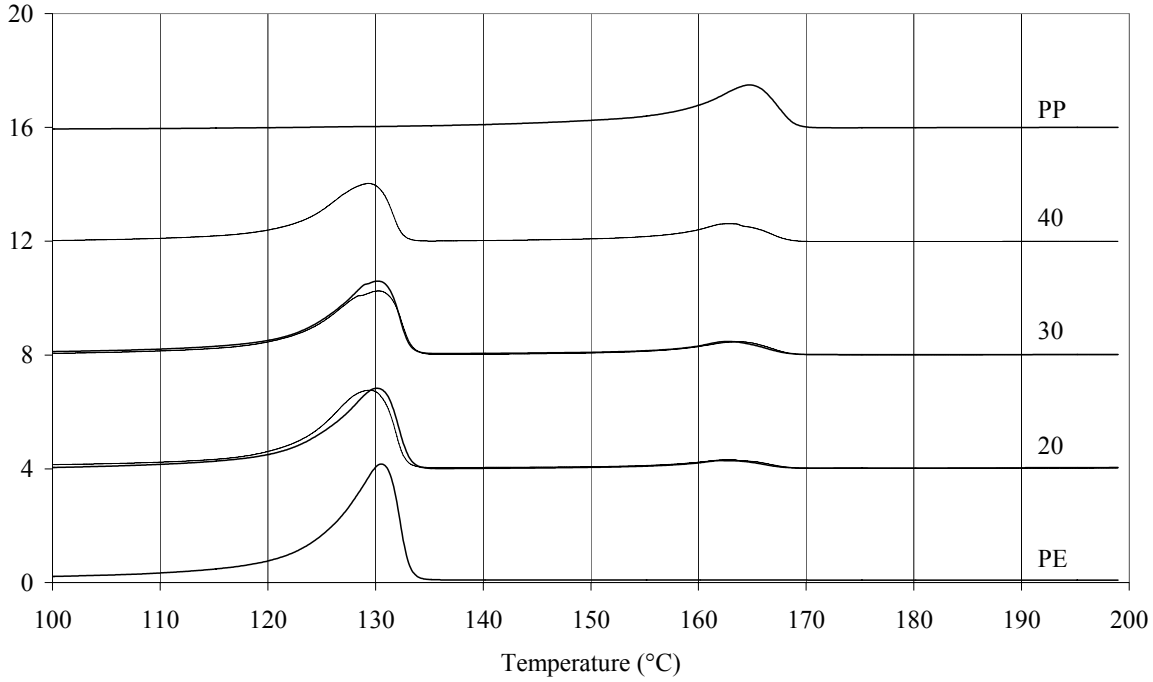

Fig. 5.14. Thermal scans of tapes extruded at mode 4 from pure and blended polymers. Solid line represents samples prepared from compounded blends and dashed line is used for hand-mixed blends.

Table V.6. Melting temperatures and heats of fusion of extrudates prepared at mode 5.

%PP	Compounded blends				Hand-mixed blends			
	PE		PP		PE		PP	
	T_m	ΔH	T_m	ΔH	T_m	ΔH	T_m	ΔH
0	-	-	-	-	131.3	187.2	-	-
20	130.8	145.1	163.6	16.0	130.1	144.7	163.0	19.1
30	129.9	133.0	162.3	25.8	130.1	127.5	163.3	25.4
40	130.4	114.9	163.0	35.1	129.7	110.9	162.8	34.0
100	-	-	-	-	-	-	164.5	101.6

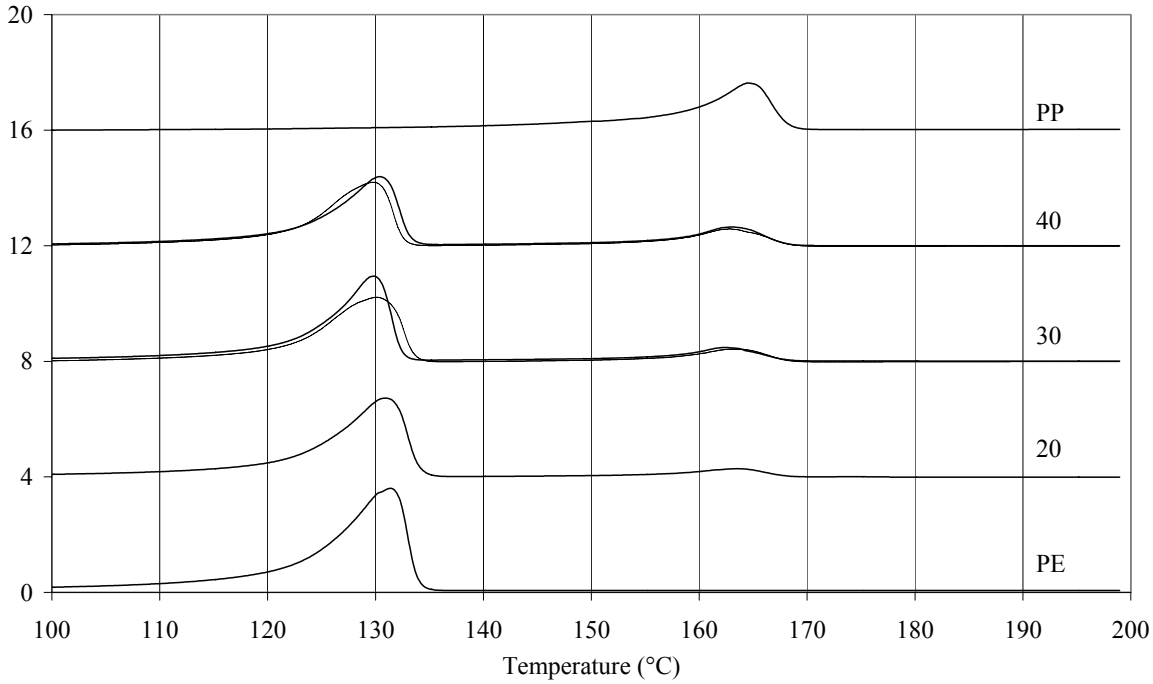

Fig. 5.15. Thermal scans of tapes extruded at mode 5 from pure and blended polymers. Solid line represents samples prepared from compounded blends and dashed line is used for hand-mixed blends.

5.1.4 Mechanical measurements

Mechanical behaviour of extruded tapes was examined using tensile testing. From stress-strain curves, values of elastic modulus and stress and strain at yield were calculated. Following figures show these characteristics as a function of phase composition.

The elastic modulus of extruded tapes as a function of phase composition is presented in Figs. 5.16-5.20. The modulus reflects the tensile behaviour of the material under a minute deformation and virtually static test conditions (strain rate 1 mm/min), i.e. in the ideal elastic region. Predominantly, values of modulus in both compounded and hand-mixed blends follow the additivity rule, i.e. they correspond to the values of blend component with respect to the phase composition. In the graphs it is displayed by virtually linear dependence of the modulus on the PP content. However, the extrudates from compounded blend containing 20 wt.% of PP show, particularly at processing modes 1-3, a significant increase in modulus, compared to the values predicted by additivity law. Moreover, under the processing modes 1-3 the modulus of these tapes achieves the highest values among extrudates prepared from both compounded and hand-mixed blends. These results indicate a synergic effect between the phases of the blend based on:

- Degree of orientation in PP phase; as proved by X-ray scattering, PP phase in extruded blends possesses significantly higher level of macromolecular orientation than the extrudate from pure material.
- Aspect ratio of microfibrils; as demonstrated by the micrographs from SEM, the finest fibrils were found in the extrudate from the blend containing 20 wt.% of PP.
- Phase cohesion; DSC measurements show a limited co-crystallization in the tapes extruded from compounded blends caused by a limited miscibility at interfaces.

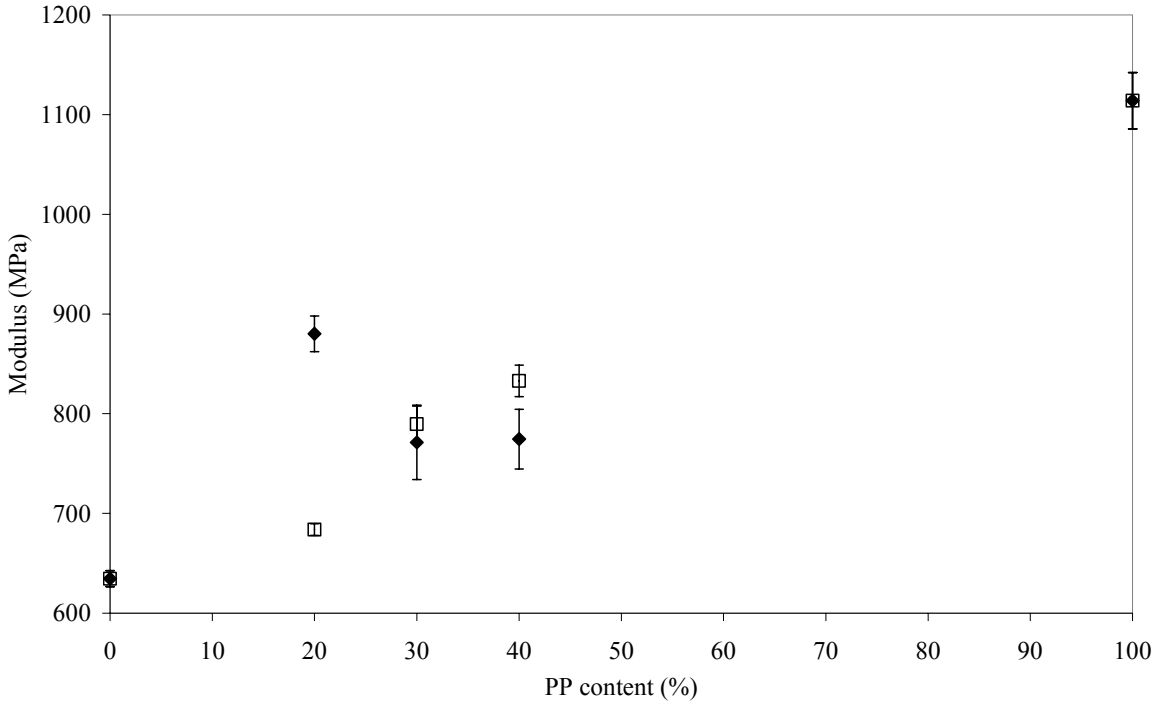

Fig. 5.16. Dependence of modulus of extrudates processed at mode 1 on composition of blends. Closed symbols stand for compounded blends and open symbols represent hand-mixed blends.

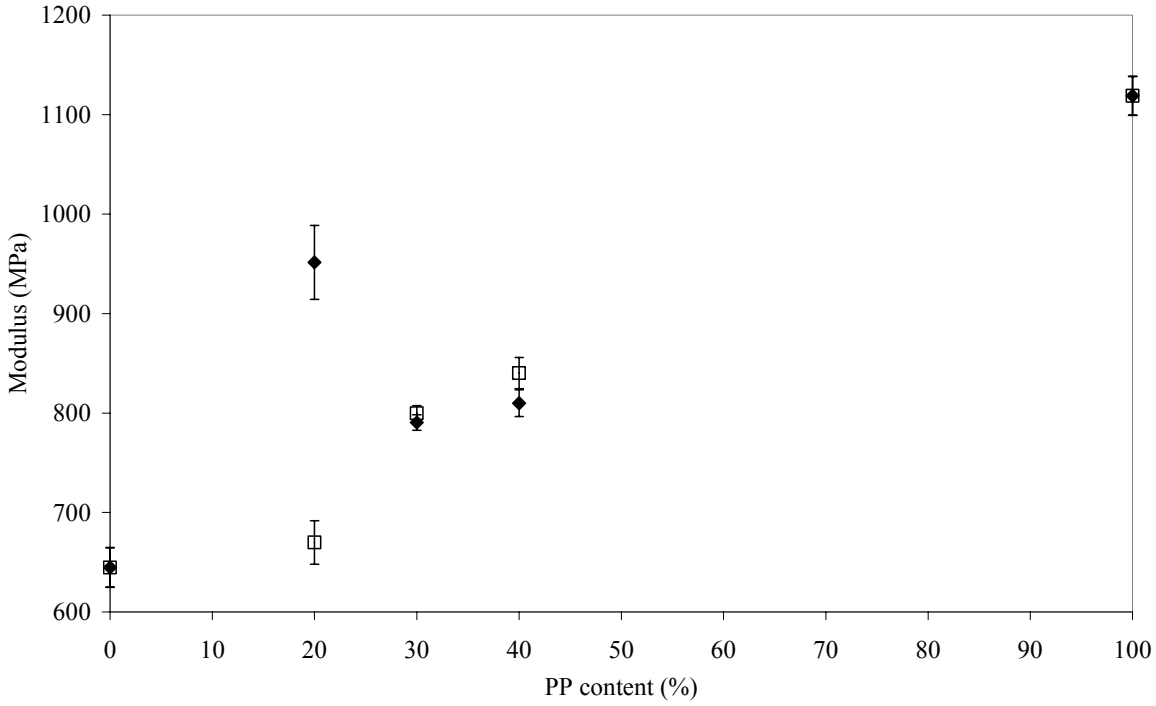

Fig. 5.17. Dependence of modulus of extrudates processed at mode 2 on composition of blends. Closed symbols stand for compounded blends and open symbols represent hand-mixed blends.

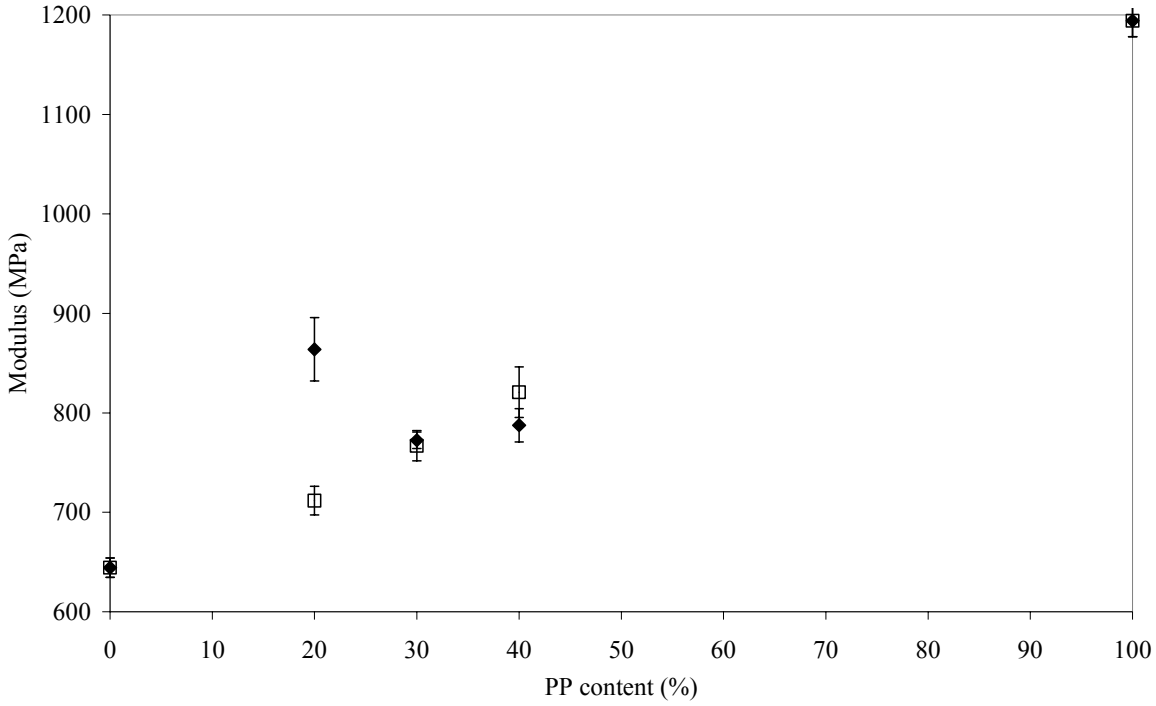

Fig. 5.18. Dependence of modulus of extrudates processed at mode 3 on composition of blends. Closed symbols stand for compounded blends and open symbols represent hand-mixed blends.

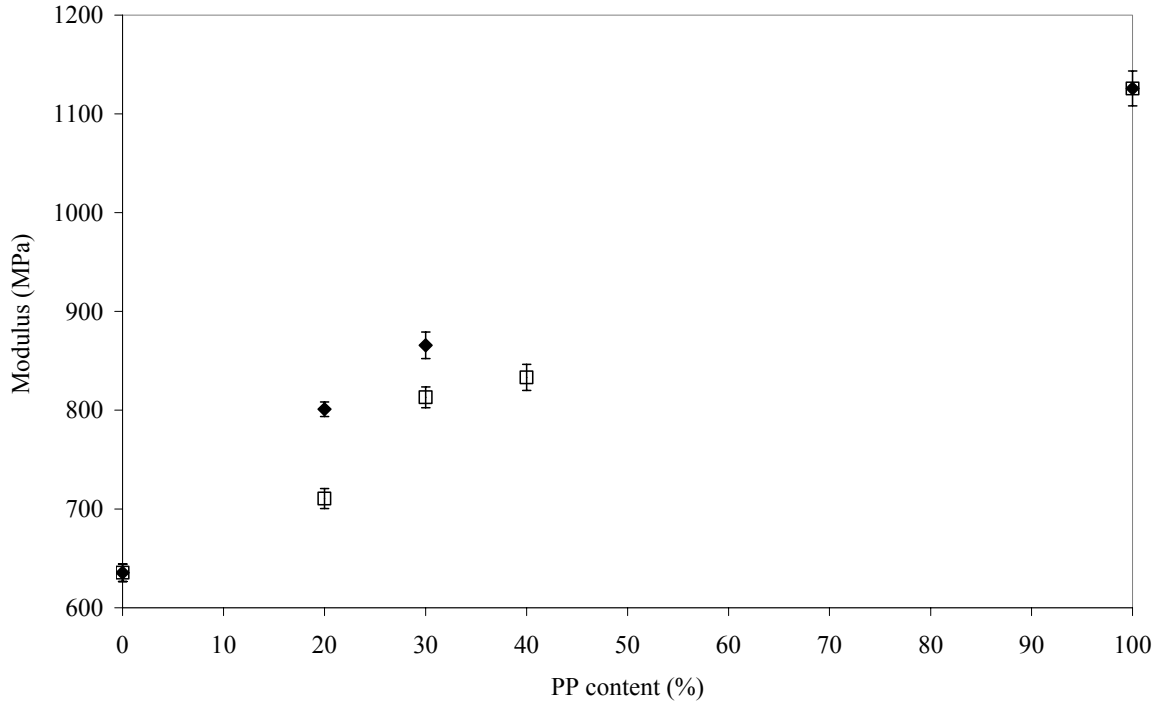

Fig. 5.19. Dependence of modulus of extrudates processed at mode 4 on composition of blends. Closed symbols stand for compounded blends and open symbols represent hand-mixed blends.

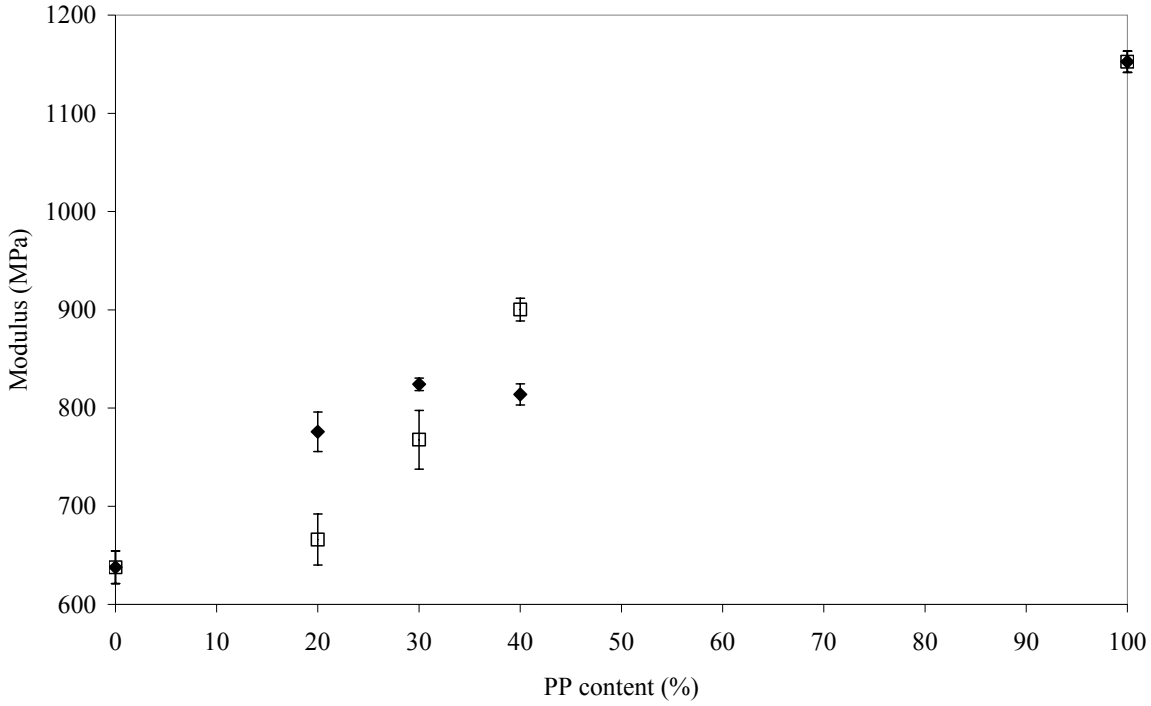

Fig. 5.20. Dependence of modulus of extrudates processed at mode 5 on composition of blends. Closed symbols stand for compounded blends and open symbols represent hand-mixed blends.

Stress and strain at yield of extruded tapes were measured to assess the potential of the material to withstand tensile stress within a semi-dynamic test (strain rate 100 mm/min). From the designing point of view, the yield stress represents the tensile strength of polymers because further deformation leads to a broad non-reversible transformation of the material during which the original structure is oriented into stress direction. Yield strain, on the other hand, can be considered the ratio of material deformability within a low-strain region. The stress and strain at yield values of all the extrudates, with respect to the phase composition and processing modes, are displayed in Figs. 5.21-5.25. In general, it can be seen that the stress at yield increases with rising amount of PP, while, at the same time, strain at yield decreases. Compared to the values predicted in accordance with additivity law, the stress at yield of tapes extruded from compounded blends at all processing conditions displays positive deviation, while the hand-mixed extrudates exhibits negative deviation. This discrepancy can be ascribed to the slightly higher level of local miscibility resulting from the process of twin-screw extrusion, as also revealed by DSC. On the other hand, the impact of the compounding on strain at yield values cannot be unambiguously assessed because of generally higher standard deviations.

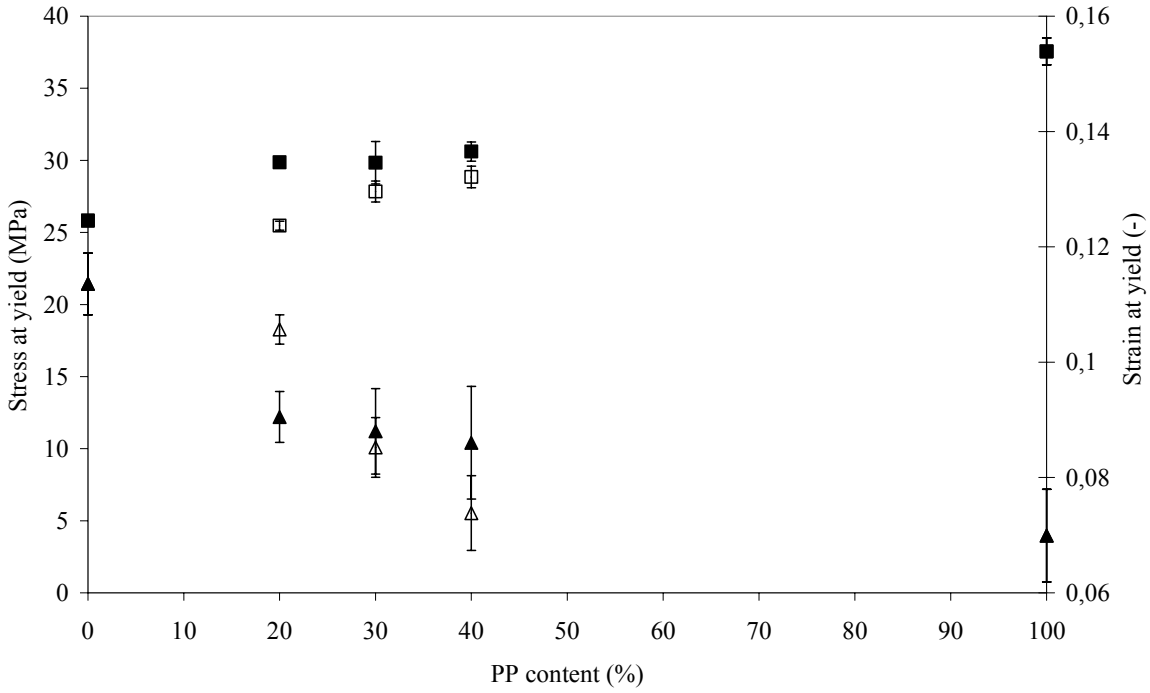

Fig. 5.21. Dependence of stress at yield (squares) and strain at yield (triangles) on blend composition of the specimen extruded at mode 1. Closed symbols stand for compounded blends and open symbols represents hand-mixed blends.

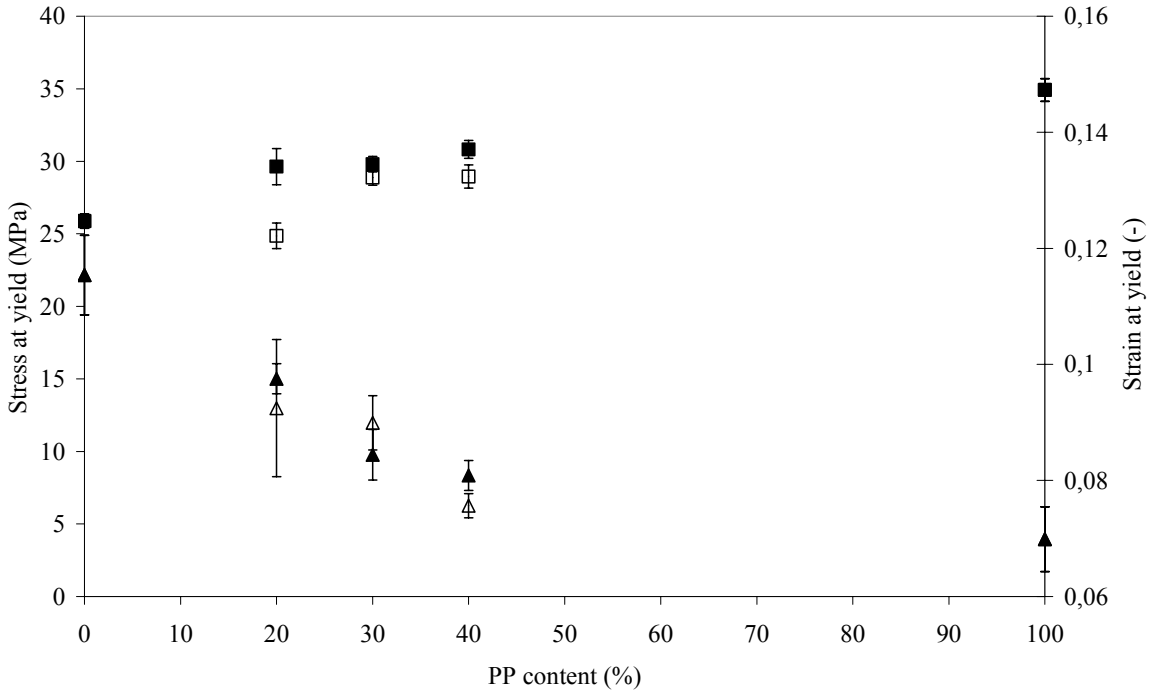

Fig. 5.22. Dependence of stress at yield (squares) and strain at yield (triangles) on blend composition of the specimen extruded at mode 2. Closed symbols stand for compounded blends and open symbols represents hand-mixed blends.

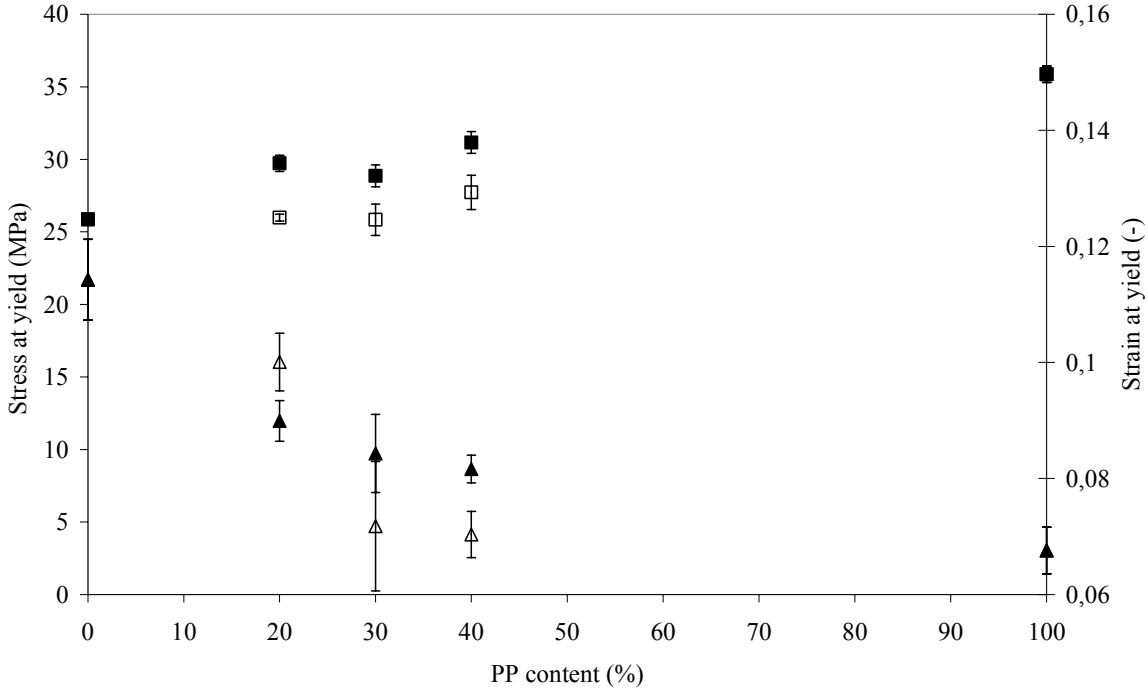

Fig. 5.23. Dependence of stress at yield (squares) and strain at yield (triangles) on blend composition of the specimen extruded at mode 3. Closed symbols stand for compounded blends and open symbols represents hand-mixed blends.

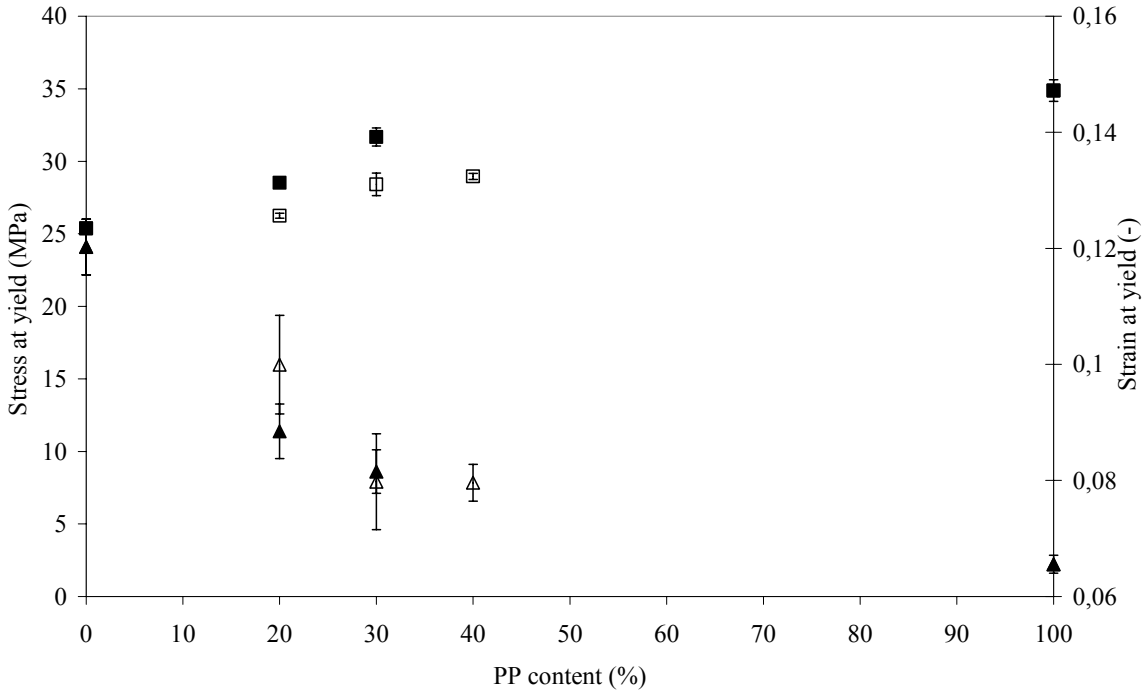

Fig. 5.24. Dependence of stress at yield (squares) and strain at yield (triangles) on blend composition of the specimen extruded at mode 4. Closed symbols stand for compounded blends and open symbols represents hand-mixed blends.

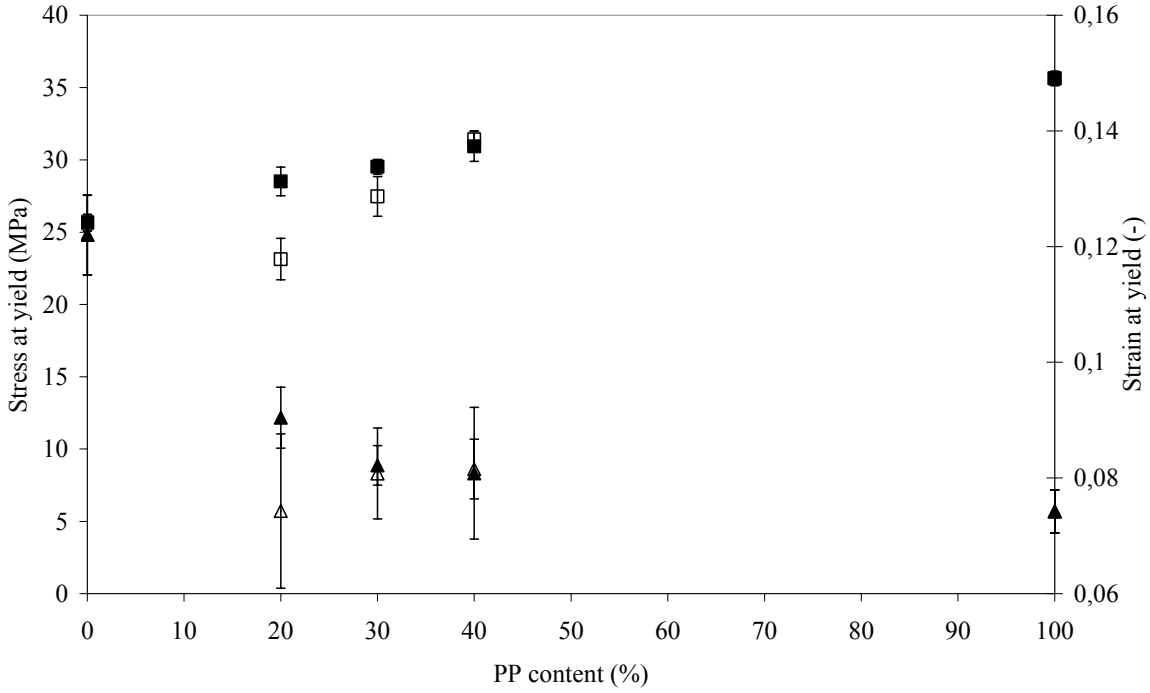

Fig. 5.25. Dependence of stress at yield (squares) and strain at yield (triangles) on blend composition of the specimen extruded at mode 5. Closed symbols stand for compounded blends and open symbols represents hand-mixed blends.

5.1.5 Rheological measurements

From processing point of view, rheological behaviour can be rated as the most important feature of the material. Results of rheological experiments performed on both pure and blended PP and PE are shown in Figs. 5.26 and 5.27. It is obvious from the Fig. 5.26 that the lowest shear viscosity in the whole measured range was obtained for pure PP. Furthermore, it can be seen that decreasing amount of PP shifts position of flow curves to higher values of shear viscosity, and, in addition, narrows the range of shear rates, in which the viscosity can be measured. In other words, due to flow instabilities, the shear viscosity of pure PE can be only measured to the shear rate of 937 s^{-1}, however, addition of 20 wt.% of PP into PE shifts critical tested shear rate to 3700 s^{-1} and, finally, the viscosity of 30/70 PP/PE blend can be measured in the whole chosen range of shear rates. In fact, this indicates that the blending of PP into PE advantageously broadens the interval of extrusion rates.

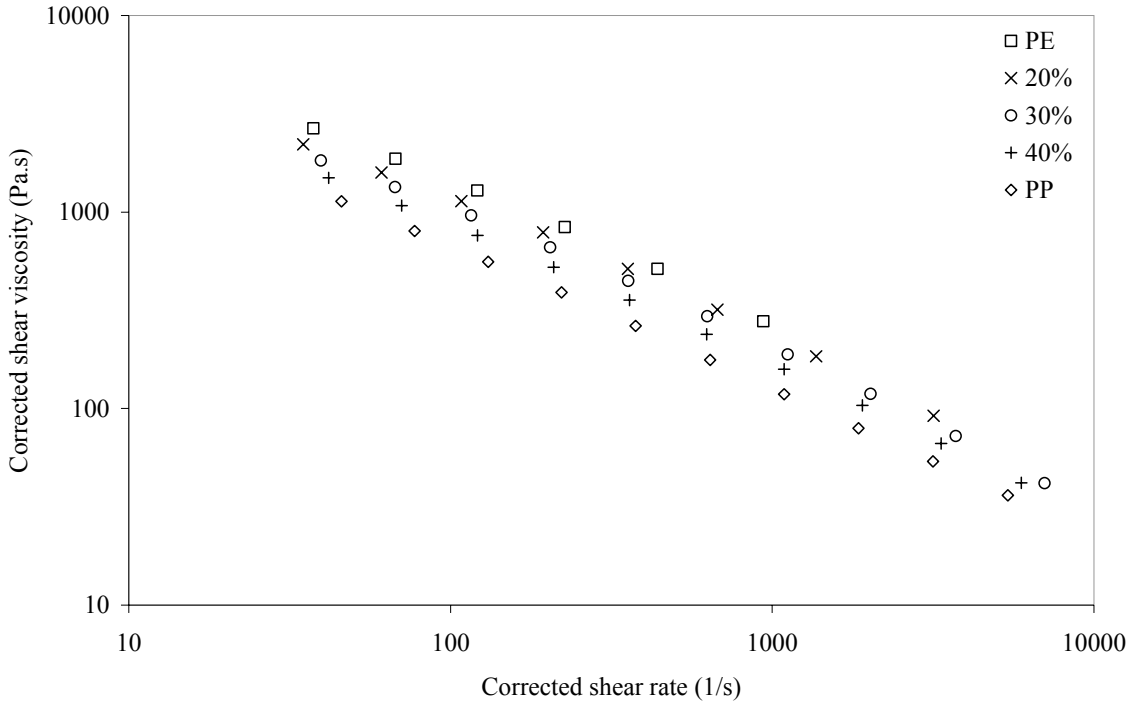

Fig. 5.26. Corrected shear viscosity as a function of corrected shear rate for compounded PE/PP blends and pure materials.

Elongational behaviour of pure materials and compounded blends is demonstrated in the Fig. 5.27. In comparison with PP, elongational viscosity of PE is more sensitive to changes in elongational rate; at low elongational rates, the viscosity of PE is higher, nevertheless,

with rising elongational rate it dramatically drops, even under the values of PP. As for the blends, it can be seen that the interval of observed elongational viscosities narrows with the rising content of PP.

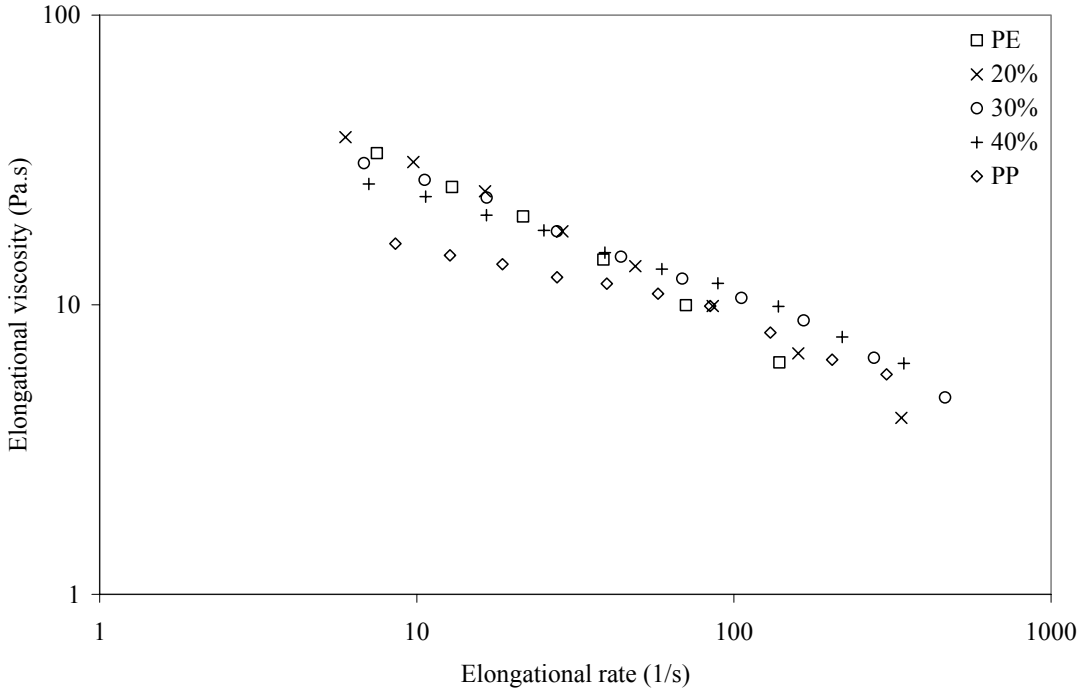

Fig. 5.27. Elongational viscosity as a function of elongational rate for compounded PE/PP blends and pure materials.

As discussed in theoretical background of the present work, the miscibility of components in the blends can be classified by log-additivity rule. For these purposes, three values of shear stresses, namely 90, 140, and 190 kPa, were chosen as exemplary levels covering the measured range. Theoretical values of viscosities calculated using log-additivity rule at chosen shear stresses are compared with experimental data in Figs. 5.28-5.30. It is obvious that the blend with 20 wt.% of PP corresponds to miscible blend behaviour, since the experimental values are similar to the values calculated from the log-additivity rule. The blend with 30 wt.% of PP appears to be partially miscible, because the values predicted from log-additivity rule are placed in the vicinity to experimental values. Blend with 40 wt.% of PP shows a large negative deviation from the log-additivity rule and consequently could be considered as an immiscible blend system. However, using the set of structure analyses it was proved that all the blends studied show two-phase structure with an utterly sporadic miscibility at interfaces. It evidences that the employment of rheology for the description of the miscibility in the blends is rather disputative.

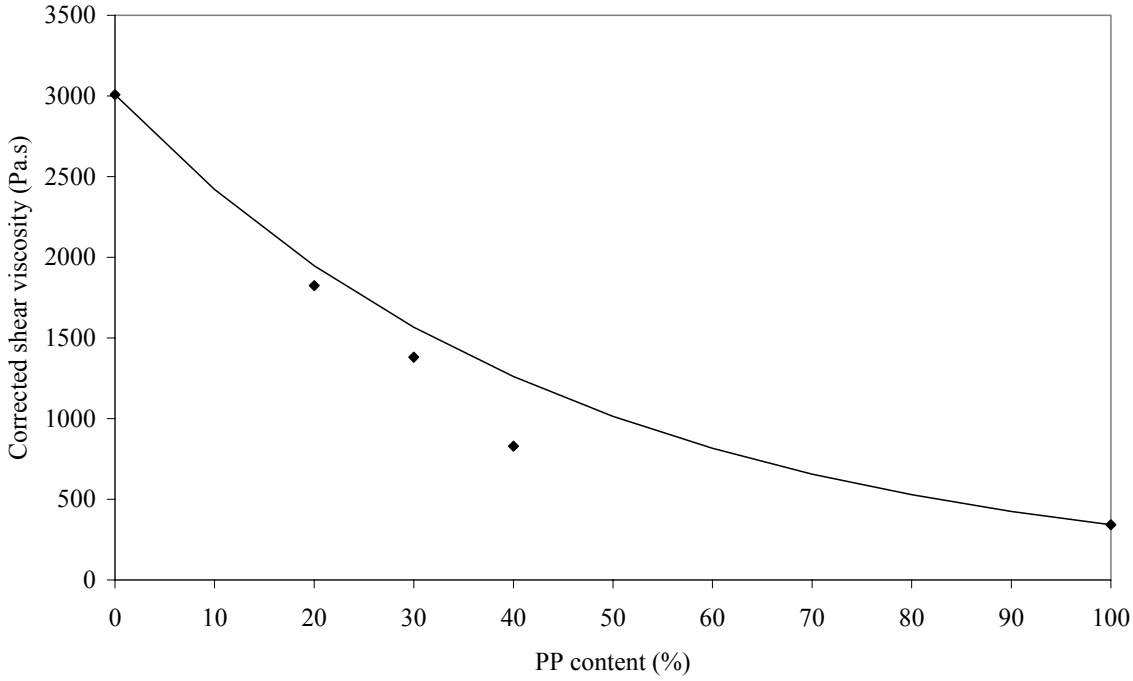

Fig. 5.28. Shear viscosity at constant shear strain of 90000 Pa as a function of blend composition. Predicted values from log-additivity rule are represented by solid line, experimental values are shown as closed symbols.

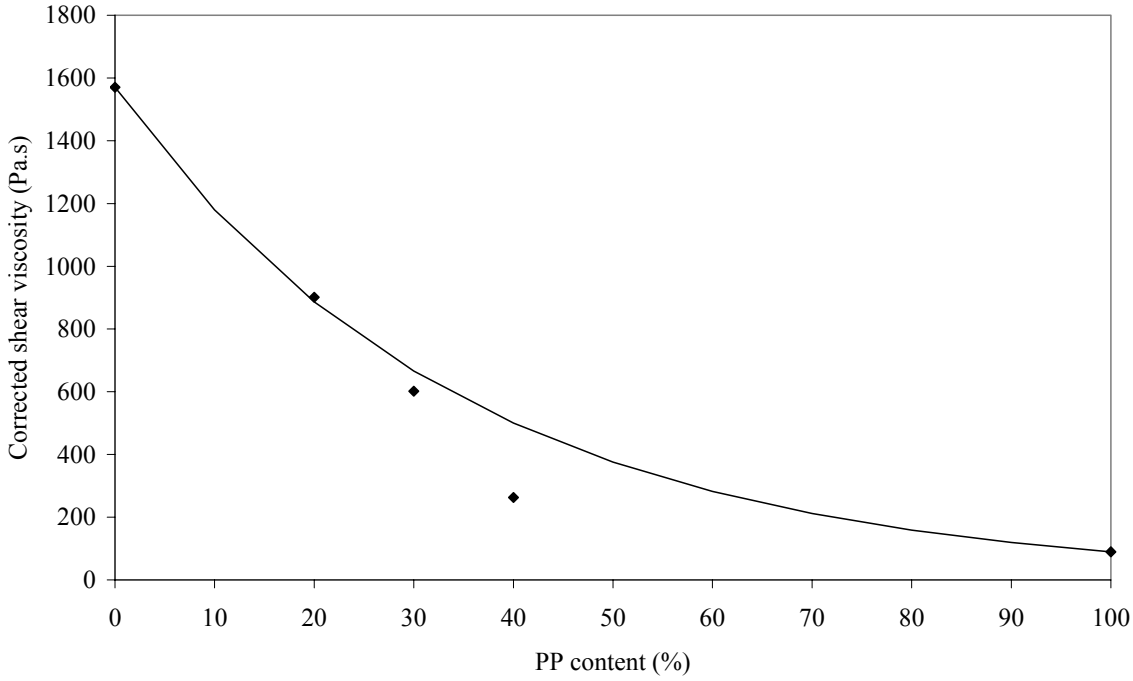

Fig. 5.29. Shear viscosity at constant shear strain of 140000 Pa as a function of blend composition. Predicted values from log-additivity rule are represented by solid line, experimental values are shown as closed symbols.

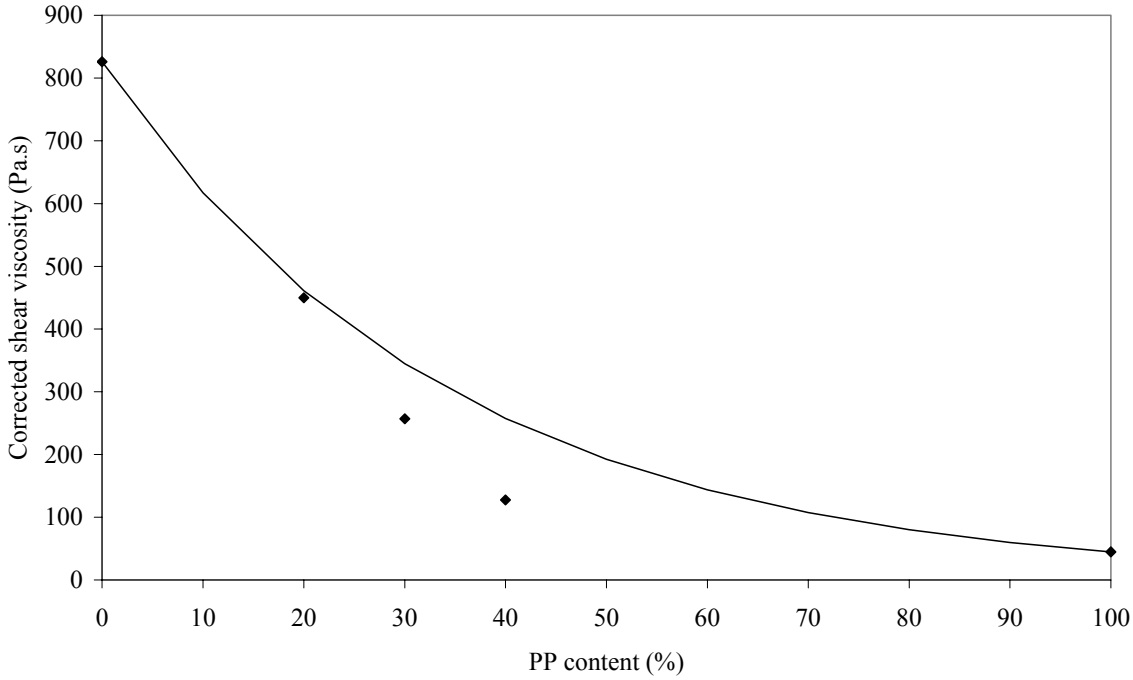

Fig. 5.30. Shear viscosity at constant shear strain of 190000 Pa as a function of blend composition. Predicted values from log-additivity rule are represented by solid line, experimental values are shown as closed symbols.

CONCLUSION

The aim of the present master thesis was preparation of microfibrillar-phase morphology in the polypropylene/polyethylene blends with polypropylene as a minority component. For these purposes an extrusion line based on conventional single-screw extruder and semihyperbolic-converging die was employed. It was proved that the formation of fibrillar structure in one processing step can be achieved using:

- Blends with various content of polypropylene; the blends with 20, 30 and 40 wt.% of PP were studied.
- Compounded and hand-mixed materials; both twin-screw extruder compounded and non-compounded materials were processed.
- Wide processing window; the conditions covered large intervals of extrusion temperatures and rates were applied.

The extruded tapes with microfibrillar morphology were examined by several methods of structure analysis and measurements of properties. Important results can be summarized as follows: (i) Wide-angle X-ray scattering showed a high orientation of PP phase in blends. The degree of orientation increases with rising amount of PP. (ii) The structure of extruded blends observed using electron microscopy gradually changes from fibril morphology to co-continuous phase structure, in respect of the PP content increase. In the compounded-blend extrudates, the aspect ratio of PP domains decreases with the rising PP amount. (iii) Differential scanning calorimetry revealed a slight shift of the melting peaks of individual phases towards themselves in compounded blends, which indicates a limited miscibility at interfaces and subsequent co-crystallization during extrusion. (iv) Values of mechanical characteristics of the blends measured by tensile testing follow generally the additivity rule. However, the extrudates from compounded blend containing 20 wt.% of PP show a significant positive deviation in elastic modulus indicating a phase synergism. (v) Rheological measurements indicated that the blending of PP into PE broadens the interval of shear rates without flow instabilities and, consequently, enables processing at higher extrusion rates. Sensitivity of elongational viscosity to the elongational rate decreases gradually with the content of PP in the blends.

REFERENCES

1) Utracki, L.A., Polymer Alloys and Blends: Thermodynamics and Rheology. Munich: Hanser Publishers, 1989.
2) Oshima, J., Sasaki, I., *Polymer News* **16**, p. 198, 1991.
3) Olabisi, O., Robeson, L.M., Shaw, M.T., Polymer-Polymer Miscibility. New York: Academic Press, 1979.
4) Utracki, L.A., Two-phase polymer systems. New York: Oxford Univ. Press, 1991.
5) Thiele, W., *Plast. Comp.* **4**, p. 23, 1981.
6) Thiele, W., *SPE Techn. Pap.* **29**, p. 127, 1983.
7) Janssen, L.P.B. M., Twin-screw Extrusion. New York: Elsevier, 1978.
8) Speur, J. A., Mavridis, H., Vlachopoulos, J., Janssen, L. P. B. M., *Adv. Polym. Techn.* **7**, p. 39, 1987.
9) Harper, Charles A., Modern plastics handbook / Modern Plastics. New York: The McGraw-Hill, 2000.
10) Thompson, W.R., Bortolini, W., Young, D.R., Davies, J.K., Polypropylene, Modern Plastics Encyclopedia 1988, reference book (M603.1). New York: McGraw-Hill, 1987.
11) McKelvey, J. M., Polymer Processing. New York: John Wiley, 1962.
12) Paul, D.R., Barlow, J.W., *J. Macromol. Sci.-Rev. Macromol. Chem.* **18**, p. 109, 1980.
13) Runt, J.P., Polymer Blends. New York: Academic Press, 1978.
14) Cowie, J.M.G., Encyclopedia of Polymer Science and Engineering, New York: Wiley Interscience, 1989.
15) Barlow, J.W. and Paul, D.R., *Polym. Eng. Sci.* **21**, p. 985, 1981.
16) Zdražilová, N., Doctoral Thesis: Rheological Response to the Structural Modification of Polymer-Based Materials. Tomas Bata University in Zlín, Faculty of Technology, 2004.
17) Xanthos, M., *Polym. Eng. Sci.* **28**, p. 1392, 1988
18) Datta, S., Lohse, D.J., Polymeric Compatibilizers – Uses and Benefits in Polymer Blends. Munich: Hanser Publishers, 1996.

19) Runt, J.P., Polymer Blends. New York: Academic Press, 1978.

20) Fortelný, I., Edice Makro **22**, p. 51, 1998.

21) Utracki, L.A., Shi, Z.H., *Polym. Eng. Sci.* **32**, p. 1824, 1992.

22) Fortelný, I., Kovář, J., Stephen, M., *J. Elastomers Plast.* **28**, p. 106, 1996.

23) Lyngaae-Jorgensen, J., Rheology of Polymer Blends. V: Polymer Blends and Alloys. London: Blackie Academic & Professional, 1993.

24) Friedrich, K., Evstatiev, M., Fakirov, S., Evstatiev, O., Ishii, M., Harrass, M., *Comp. Sci. Tech.* **65**, p. 107, 2005.

25) Tjong, S. C., *Mater. Sci. Eng.* **41**, p.1, 2003.

26) Han, C. D., Multiphase Flow in Polymer Processing. New York: Academic Press, 1981.

27) Evstatiev, M., Fakirov, S., *Polymer* **33**, p. 877, 1992.

28) Fakirov, S., Evstatiev, M., Petrovich, S., *Macromolecules* **26**, p. 5219, 1993.

29) Fakirov, S., Evstatiev, M., *Adv. Mater.* **6**, p. 395, 1994.

30) Aharoni, S.M., *Int. J. Polym. Mater.* **38**, p. 173, 1997.

31) Fakirov, S., Apostolov, A., Denchev, Z., Stribeck, N., Evstatiev, M., Friedrich, K., *J. Macromol. Sci.* **40**, p. 935, 2001.

32) Fakirov, S., Evstatiev, M., Friedrich, K., Polymer blends. New York: J. Wiley and Sons, 2000.

33) Evstatiev, S., Fakirov, S., Friedrich, K., In: Cunha A.M., Fakirov, S., editors. Structure development during polymer processing. London: Kluwer Academic Publisher; 2000.

34) Manas-Zloczower, I., Tadmor, Z., Mixing and compounding of polymers: theory and practice. Munich: Hanser Publisher, 1994.

35) Bridson, J.A., Plastics materials. Oxford: Butterworth-Heinemann, 1999.

36) Severin, N., Doctoral Thesis: Molecular Dynamics Simulations of Polymers and Micelles at Interfaces. Humbolt-Universität zu Berlin. Mathematisch-Naturwissenscheftlichen Fakultät I, 1998.

37) Keller, A., *Polymer* **41**, p. 8751, 2000.

38) Basset, D.C., Hodge, A.M., Olley, R.H., *Proc. R. Soc. Lond. Ser. A* **377**, p. 39, 1981.

39) Neway, N., Doctoral Thesis: The Influence of Morphology on the Transport and Mechanical Properties of Polyethylene. Royal Institute of Technology, 2003. Available on:http://www.lib.kth.se/Sammanfattningar/neway031212.pdf

40) Woodward, A.E., Understanding the Polymer Morphology. Munich: Carl Hanser Verlag, 1995.

41) Maier, C., Calafut, T., Polypropylene, the definitive user's guide and databook. Cosi: Plastic Design Library, 1998.

42) Brandrup, J., Immergut, E. H., Polymer Handbook. New York: J. Willey and Sons, 2003.

43) Mleziva, J., Šňupárek, J., Polymery – Výroba, struktura, vlastnosti a použití. Praha: Sobotáles, 2000.

44) Portnoy, R.C., *Medical Plastics and Biomaterials* **1**, p. 4347, 1994.

45) Ouederni, M., Phillips, P.J., Effect of a Nucleating Agent on the Fracture Toughness of Isotactic Polypropylene. *ANTEC 1996 Plastics*, 1996.

46) Campbell, D., White, J.R., Polymer characterization. New York: Chapman and Hall, 1989.

47) Levi, K., Doctoral Thesis: On the Determination of the Crystalline Fraction of Copolymer Blends from Wide Angle X-Ray Spectroscopy (WAXS). Washington and Lee University, 2003. Available on: http://www.thecollege.wlu.edu/research_service/RELee/Physics2003/LeviFinal.asp.htm

48) www.mos.org/sln/SEM/

49) Hatakeyama, T., Quinn, F.X., Thermal Analysis: Fundamentals and Applications to Polymer Science. New York: J. Wiley and Sons, 1995.

50) Diamond Differential Scanning Calorimeter (DSC) - High Sensitivity Thermal Analysis, 2003. Available on: http://las.perkinelmer.com/content/RelatedMaterials/006887_01.pdf

51) Moore, D.R., Turner, S., Mechanical evaluation strategies for plastics materials. Cambridge: Woodhead Publishing Limited, 2001.

52) Macosko, C.W., Rheology: Principles, Measurements, and Applications. New York: VCH Publishers, 1994.

53) Treloar, L.R.G., The Physics of Rubber Elasticity, Oxford: Clarendon Press, 1975.

54) Pandmanabhan, M., Macosko, C.W., *Rheol. Acta* **36**, p. 144, 1997.

55) Metzner, A.B., Metzner, A.P., *Rheol Acta* **9**, p. 171, 1970.

56) Cogswell, F.N., *Polym. Eng. Sci.***12**, p. 64, 1972.

57) Binding, D.M., *J. Non-Newtonian Fluid. Mech.* **27**, p. 173, 1988.

58) Binding, D.M., *J. Non-Newtonian Fluid. Mech.* **41**, p. 27, 1991.

59) Binding, D.M., Techniques in Rheological Measurement. New York: Chapman and Hall, 1993.

60) Chuang, H.K., Han, C.D., Polymer Blends and Composites in Multiphase Systems. New York: American Chemical Society, 1984.

61) Utracki, L.A., *J. Rheol.* **35**, p. 1615, 1991.

62) Utracki, L.A., *Polym. Eng. Sci.* **23**, p. 602, 1983.

63) Han, C.D., Multiphase Flow in Polymer Processing. New York: Academic Press, 1981.

64) Trotignon, J.P., Lebrun, J.L., Verdu, J., *Plast. Rubber Process. Appl.* **2**, p. 247, 1982.

LIST OF SYMBOLS

A	crystalline orientation
a.u.	arbitrary unit
d	interplanar distance
D_0	short capillary diameter
D_B	barrel diameter
D_L	long capillary diameter
DSC	differential scanning calorimetry
I	total integral intensities
I_C	integral intensities diffracted by a crystalline part
$I_{(110)}$	intensity of (110) reflection
$I_{(111+041)}$	intensity of (110+041) reflection
$I_{(040)}$	intensity of (040) reflection
L_0	short capillary length
L_L	long capillary length
LCP	liquid crystalline polymer
MFC	microfibrillar-reinforced composite
n	power-law index
O	degree of orientation
P_0	pressure drop measured orifice capillary
P_L	pressure drop measured with long capillary
PE	linear high-density polyethylene
PO	polyolefins
PP	isotactic polypropylene
Q	volume flow rate

R	capillary radius
SEM	scanning electron microscopy
TEM	transmission electron microscopy
T	temperature
T_{cal}	temperature of calibration zone
T_{con}	temperature of converging zone
T_{cyl}	temperature of cylinder zone
T_g	glass transition temperature
T_m	melting temperature
T_{pump}	temperature of gear pump
w_i	weight fraction of ingredient "i" in the blend
wt.%	weight percent
X_C	crystallinity
ΔG_m	free energy of mixing
ΔH_m	enthalpy change of mixing
ΔH	heat of fusion
ΔS_m	entropy change of mixing
$\dot{\varepsilon}$	elongational rate
ϕ_2	volume fraction of the second component
$\dot{\gamma}_a$	apparent shear rate
$\dot{\gamma}$	shear rate
η	corrected shear viscosity
η_e	elongational viscosity
η_i	viscosity of ingredient "i" in the blend
λ	wavelength

θ	angle of diffraction
σ_e	elongational stress
τ	corrected shear stress

LIST OF FIGURES

LIST OF TABLES